WILEY

Cladistics

Cladistics 40 (2024) 577–597

doi: 10.1111/cla.12595

A targeted gene phylogenetic framework to investigate diversification in the highly diverse yet geographically restricted red devil spiders (Araneae, Dysderidae)

Silvia Adrián-Serrano*[a,b], Martina Pavlek[a,b,c,d] and Miquel A. Arnedo[a,b]

[a]*Departament Biologia Evolutiva, Ecologia i Ciències Ambientals, Universitat de Barcelona, Av. Diagonal 645, E-08028 Barcelona, Spain;* [b]*Institut de Recerca de la Biodiversitat (IRBio), Universitat de Barcelona, Av. Diagonal 645, E-08028 Barcelona, Spain;* [c]*Ruđer Bošković Institute, Bijenička cesta 54, Zagreb, Croatia;* [d]*Croatian Biospeleological Society, Roosveltov trg 6, Zagreb, Croatia*

Received 12 March 2024; Revised 12 June 2024; Accepted 10 July 2024

ABSTRACT

The family Dysderidae is a highly diverse group of nocturnal ground-dwelling and active-hunter spiders. Dysderids are mostly restricted to the Western Palearctic, and particularly rich and abundant around the Mediterranean region. Interestingly, the distribution of species richness among its 24 genera and three subfamilies is highly biased—80% of its 644 documented species belong to just two genera, *Dysdera* (326) and *Harpactea* (211). Dysderidae provides an excellent study case for evolutionary and ecological research. It includes cases of trophic specialization, which are uncommon among spiders, and exhibit other remarkable biological (e.g. holocentric chromosomes), behavioural (e.g. cryptic female choice), evolutionary (e.g. adaptive radiation) and ecological features (e.g. recurrent colonization of the subterranean environment). The lack of a quantitative hypothesis on its phylogenetic structure has hampered its potential as a testing ground for evolutionary, biogeographical and ecological hypotheses. Here, we present the results of a target, multi-locus phylogenetic analysis, using mitochondrial (cox1, 16s and 12s) and nuclear genes (h3, 28s and 18s), of the most exhaustive taxonomic sample within Dysderidae (104 spp.) to date and across related families (Synspermiata) (83 spp.). We estimate divergence times using a combination of fossil and biogeographic node calibrations and use this timeline to identify shifts in diversification rates. Our results support the monophyly of the Dysderidae subfamilies Rhodinae and Dysderinae but reject Harpacteinae as currently defined. Moreover, the clades recovered within Harpacteinae do not support its current taxonomy. The origin of the family most likely post-dated the break-up of Pangea, and cave colonization may be older than previously considered. After correcting for the taxonomic artefacts, we identified a significant shift in diversification rates at the base of the genus *Dysdera*. Although the unique coexistence of specialist and generalist diets within the lineage could be suggested as the potential driver for the rate acceleration, further quantitative analyses would be necessary to test this hypothesis.

Introduction

The spider family Dysderidae C.L. Koch, 1837, also known as red devil spiders or dysderids, is a group of medium-size ground dwelling spiders (Fig. 1), usually found in warm and wet, but not damp, shaded ground habitats. Most species are nocturnal wandering hunters that spend daylight in silk retreats, in the leaf-litter, under stones or dead logs (Řezáč et al., 2007). Dysderids are mostly found in forested areas, but they are not uncommon in open habitats. They are also among the most frequent and diverse groups of spiders in Mediterranean caves (Deltshev, 1999; Culver and Sket, 2000; Ribera, 2004; Mammola et al., 2018). Some species have evolved morphological adaptations to the underground habitat (i.e. troglobiomorphism), including eye reduction, appendage elongation and depigmentation.

*Corresponding author:
E-mail address: silviaadrian@ub.edu

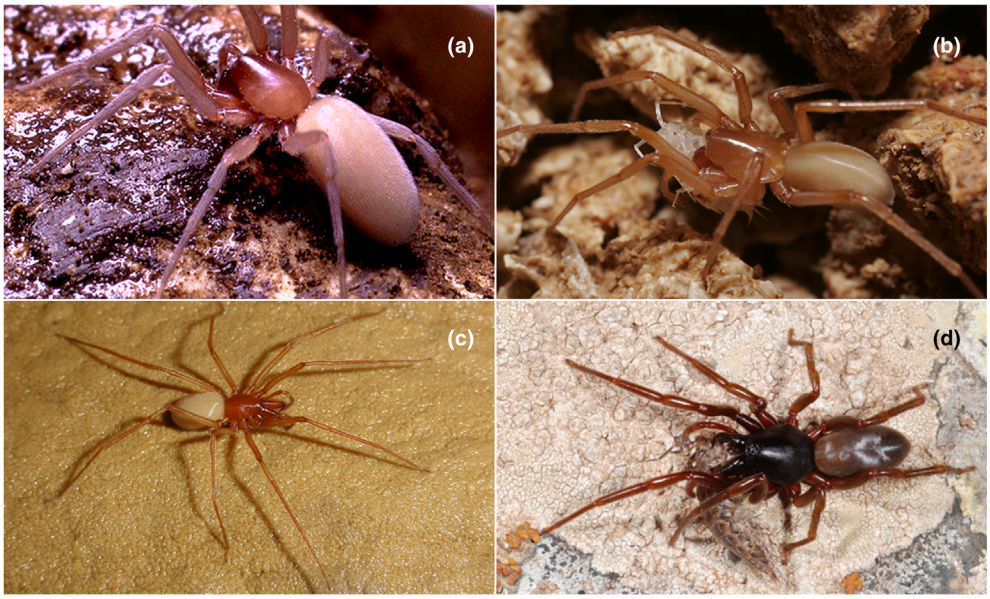

Fig. 1. Representatives of the family Dysderidae. (a) *Speleoharpactea levantina* (Harpacteinae), credit A. Sendra; (b) *Stalagtia hercegovinensis* (Harpacteinae), credit Jana Bedek; (c) *Parastalita stygia* (Rhodinae), credit Fulvio Gasparo; (d) *Dysdera verneaui* (Dysderinae), credit Pedro Oromí.

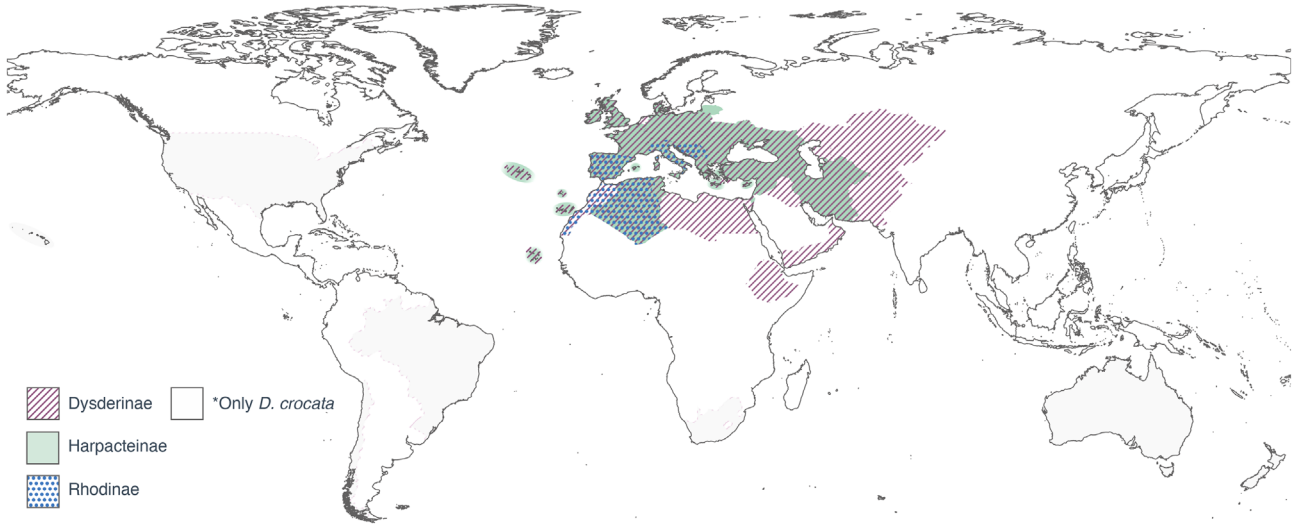

Fig. 2. Dysderidae family distribution by subfamily. Areas where the only species present is the synanthropic *Dysdera crocata* are shown apart. Distribution information obtained from the World Spider Catalogue (World Spider Catalog, 2023).

Dysderidae is mostly restricted to the Western Palearctic, but it is particularly diverse around the Mediterranean Basin (Fig. 2). Its geographic distribution extends from the European and North African Atlantic coast eastward as far as Kashmir, southward to the dry belt that runs from the Arabian Desert to the Sahara and northward to about parallel 58°, above which winters become too harsh to complete species development. Most genera have relatively narrow distributions that largely correspond to the main Mediterranean peninsulas. However, the distribution ranges of the genera *Harpactea* Bristowe, 1939 and *Dysdera* Latreille, 1804, match or, in the case of *Dysdera*, extend beyond those of the rest of the family. *Dysdera* has managed to colonize the Macaronesian archipelagoes, a group of oceanic islands of volcanic origin on the eastern side of the North Atlantic Ocean. In these islands, *Dysdera* underwent a major diversification process (e.g. more than 50 endemic species in the Canary Islands (Arnedo et al., 2001) and 12 in the Madeiran Archipelago (Crespo et al., 2021a)). Moreover, the synanthropic species *Dysdera crocata*

C.L. Koch, 1839 has been introduced all over the world (Cooke, 1965) (Fig. 2), and it is presently considered an alien invasive species (http://www.issg.org/), although its effect on endemic invertebrates that inhabit similar niches remains unknown.

Dysderidae is part of the superfamily Dysderoidea, along with the worldwide distributed families Segestriidae Simon, 1893 and Oonopidae Simon, 1890 and the Gondwanan Orsolobiidae Cooke, 1965. The superfamily monophyly is supported by the advanced location of posterior tracheal spiracles, immediately behind the spiracles of the book lungs, and the development of the posterior wall of the bursal cavity of the female vulva (Forster and Platnick, 1985). The four families are also characterized by unusual holocentric chromosomes, which could constitute an additional synapomorphy (Král et al., 2006). Cladistic analyses of morphological data supported both the monophyly of the superfamily and the sister relationship between Oonopidae and Orsolobidae, but failed to resolve relationships among the remaining families (Platnick et al., 1991; Ramírez, 2000).

The phylogenetic position of Dysderidae has also been scrutinized using phylogenomic data in the context of resolving interfamily relationships within spiders. Most studies agreed in supporting Dysderoidea and its sister group relationship with Caponiidae Simon, 1890 and Trogloraptoridae Griswold, Audisio & Ledford, 2012 (Garrison et al., 2016). However, they disagreed in considering either Orsolobidae (Fernández et al., 2018; Michalik et al., 2019; Kulkarni et al., 2021; Ramírez et al., 2021) or Oonopidae as sister to Dysderidae (Kallal et al., 2021). Surprisingly, recent analyses using ultra-conserved elements have recovered a sister group relationship of Orsolobidae and Segestriidae, which are in turn sister to Dysderidae, albeit with low support (Kulkarni et al., 2023).

Although the monophyly of Dysderidae has never been called into question, it has never been rigorously tested either. The polarity of the characters generally used to diagnose the family (labium long; parallel maxillae, longer than labium; chitinous projections of lateral areas of the sternum encircling the coxae, monopectinate claws, autospasy between coxa and trochanter) have never been discussed. The only putative synapomorphy of the family is the presence of an extremely elongated acrosomal vacuole in the sperm cells (Michalik et al., 2004).

The family currently includes 644 species, ranking 18th among the 135 spider families (World Spider Catalog, 2023). Dysderid species are grouped in 24 genera and three subfamilies, Harpacteinae, Rhodinae and Dysderinae, which are defined by the shape of the frontal margin of the sternum and the presence of a scopula, a tuft of dense hairs, replacing the middle tarsal claw (Cooke, 1965; Deeleman-Reinhold and Deeleman, 1988). The shared presence of a wide labial sternum border suggests that Rhodinae and Dysderinae may be more closely related.

The distribution of species diversity among dysderid genera, on the other hand, is highly skewed. Most of the genera include barely a dozen species, seven of them being monotypic. However, *Harpactea* (211 spp.) and *Dysdera* (326 spp.) are among the most species-rich genera of spiders and make up more than 80% of the family diversity (World Spider Catalog, 2023). Several species groups have been proposed to further classify the diversity of these two genera (Alicata, 1966; Brignoli, 1978; Deeleman-Reinhold, 1993), and according to some authors the species groups within *Harpactea* may deserve full genus status (Alicata, 1966; Deltshev, 2011).

To date, most phylogenetic studies within the family have largely focused on particular genera or species groups (Arnedo et al., 2001, 2007, 2009; Macías-Hernández et al., 2008, 2010; Řezáč et al., 2018; Crespo et al., 2021a, b). The only subfamily to have been well represented in molecular phylogenies is Dysderinae, which has been found to be monophyletic, and its internal structure is well supported (Bidegaray-Batista and Arnedo, 2011; Bidegaray-Batista et al., 2014). Conversely, the other two subfamilies have only been represented by few representatives and studies have yielded contrasting results. Wheeler et al. (2017) found Harpacteinae to be sister to Dysderinae based on a Sanger multi-locus approach, while Adrián-Serrano et al. (2021) recovered Rhodinae as sister to Harpacteinae using mitogenomic data. Platania et al. (2020) conducted a Sanger mutli-locus analysis on a more extended taxonomic sampling within Harpacteinae, which revealed polyphyly of the subfamily, with one lineage being closer to Rhodinae and the other one to Dysderinae.

Dysderids are exceptionally conservative in terms of morphology and ecology, and intrageneric diagnostic characters are almost exclusively restricted to genitalia. As haplogyne spiders, male palp and female vulva are presumed to be simple. However, the dysderid reproductive system shows several peculiarities. The copulatory bulb exhibits a large variation that spans from the all-fused, pyriform bulb of *Harpactocrates* Simon, 1914 to well-developed distal haematodocha and tegular and embolic apophyses, as in *Dysdera*. On the other hand, the typical single-duct vulva of haplogyne spiders has been suggested to favour first male sperm priority (Austad, 1984). However, the vulval structures of some dysderids appear rather complex (Cooke, 1966; Uhl, 2000a; Burger and Kropf, 2007), which has been interpreted as evidence of cryptic female choice and/or conflict between the sexes over removal or repositioning of stored sperm within the female (Uhl, 2000b). Finally, dysderid spiders are also known to possess a peculiar sperm transfer form known as synspermia,

characterized by fused spermatozoa surrounded by a secreted sheath (Michalik and Ramírez, 2014). The presence of synspermia is shared with other families and constitutes the synapomorphy of the group known as Synspermiata.

Some dysderids are also peculiar regarding their feeding behaviour. Spiders, including dysderids, are usually considered euryphagous predators, i.e. they consume a large variety of prey. However, some species within the species rich genus *Dysdera* have specialized on feeding on woodlice (Crustacea, Isopoda, Oniscoidea). Woodlice are usually avoided by generalist predators because of their morphological (e.g. a hard dorsal armour), chemical (e.g. repugnatorial glands) and behavioural (e.g. rolling or clinging) defences (Tuf and Ďurajková, 2022). Nonetheless, specialist predators, including some species of *Dysdera*, grow faster and more efficiently while feeding on woodlice (Pekár et al., 2016). *Dysdera* species specialized in feeding on woodlice have evolved modified chelicerae with different morphologies (elongated, concave or flattened), leading to different capture tactics (Řezáč et al., 2008). The degree of prey specialization correlates with the degree of phenotypic modification and physiological nutritional adaptation (Řezáč and Pekár, 2007; Bellvert et al., 2023). Interestingly, it has recently been shown that prey specialization evolved multiple times independently within the diversification of *Dysdera* in the Canary Islands (Řezáč et al., 2021; Bellvert et al., 2023). Moreover, the numerous species with overlapping distributions in the archipelago tend to diverge in phenotypic characters, which hints at the putative key role of intraspecific competition in structuring local communities (Arnedo et al., 2007).

Because of their peculiar anatomy, contrasting ecology, high diversity and circumscribed distribution, Dysderidae provide an excellent testing ground to evaluate competing hypotheses on species diversification and its drivers. The extremely biased distribution of species richness across its genera, for instance, provides ample opportunities for investigating external and intrinsic factors responsible for shifts in diversification rates. Similarly, the family is exceptionally well suited for the study of insular evolution and offers a comparative framework to study the tempo and mode of evolution between islands and continents. Moreover, the restricted distributions of most genera coupled with the well-known geochronology of the Mediterranean region provide multiple biogeographic calibrations to infer time-stamped phylogenetic trees (Bidegaray-Batista and Arnedo, 2011), which helps to alleviate the limitations of a sparse fossil record inherent to many family level relationships with spiders and other arthropods.

Central to the study of the evolutionary questions posed by the family is the inference of a thoroughly sampled, well-supported phylogeny. Here, we present the results of a Sanger multi-locus phylogenetic analysis, using mitochondrial (cox1, 16s and 12s) and nuclear genes (h3, 28s and 18s) of an extensive taxonomic sample within Dysderidae and across related families in the clade Synspermiata. We further combined fossil and biogeographic calibrations to estimate a timeline of the evolution of the family and we used this information to identify putative shifts in the diversification rates of the group.

Materials and methods

Taxon sampling

Taxonomic information and the localities of specimens analysed in the present study are listed in Table S1. We included all known genera within Dysderidae, except for the monotypic genera *Stalitochara* Simon, 1913 and *Rhodera* Deeleman-Reinhold, 1989, which may actually be junior synonyms of *Dysdera* (Ribera and Arnedo, 1994). We sampled most of the species groups proposed in the literature within the species-rich genera *Dysdera* and *Harpactea*, and paid special attention to cave-dwelling representatives within Rhodinae and Harpacteinae. Our outgroup included representatives of all remaining families within the clade Synspermiata, to which the Dysderidae belong (Michalik and Ramírez, 2014), except for Psilodercidae and Telemidae. We rooted all trees assuming the families Hypochilidae Marx, 1888, and Filistatidae Ausserer, 1867 are the sister-groups to Synspermiata, as recovered in recent phylogenomic analyses of spiders (Garrison et al., 2016; Fernández et al., 2018; Shao and Li, 2018; Kallal et al., 2021).

Most Dysderidae specimens were collected in the field by the authors, with the help of some colleagues. Several Harpacteinae and Rhodinae specimens collected in the Dinaric Alps were kindly provided by the Croatian Biospeleological Society. Additional material was kindly provided by many colleagues. Most outgroup sequences were downloaded from the NCBI (National Center of Biotechnology Information) public database (Geer et al., 2010).

Molecular procedures

Specimens collected in the field were fixed in 95% ethanol and stored at −20 °C at the Universitat de Barcelona. In some cases, we had to rely on specimens from 75% ethanol collections, which yielded reasonable quality DNA for times of storage shorter than 5 years. Vouchers have been deposited at the Centre de Recursos de Biodiversitat Animal (http://www.ub.es/crba/) in Barcelona, Spain, and at the Croatian Biospeleological Society collection (https://www.hbsd.hr/?lang=en) in Zagreb, Croatia.

We removed genitalia as vouchers and extracted total genomic DNA from the second and third right legs or, if smaller than 5 mm, from the whole specimen. We used two different commercial kits: the Speedtools Tissue DNA Extraction Kit (Biotools) for general extractions and the QIAamp DNA Micro Kit (Qiagen) for old or poorly preserved samples (e.g. 75% ethanol stored at room temperature).

DNA fragments of six genes were targeted in the present study, three mitochondrial, namely cytochrome c oxidase subunit I (cox1)

and the large (16s) and small (12s) ribosomal subunits, and three nuclear, namely histone 3 (h3) and the large (28s) and small (18s) ribosomal subunits. Sequences of all target genes were obtained in-house, except for the 12s, which were downloaded from NCBI. DNA amplification was carried out in a 20 μL reaction volume, including 5 μL of MyTaq Red Reaction Buffer from Bioline (which contains the four types of dNTPs (5 mM), $MgCl_2$ (15 mM), stabilizers and enhancers), 0.2 μL of both forward and reverse 0.1 μM primers, 0.2 μL of MyTaq Red DNA Polymerase from Bioline, 2–4 μL of genomic DNA (depending on the quality of the sample) and ultrapure Milli-Q water to make up the final volume. The primer sequences used in the amplification and subsequent sequencing are listed in Table S2. The PCR conditions set for the amplification of each gene and additional details about primer combinations and their performance are included as Supporting Information (Tables S3 and S4).

Unpurified PCR products were Sanger sequenced in both directions at Macrogen Inc. (Madrid, Spain), using the same amplification primers. Raw sequences were assembled, edited and handled using the software Geneious v11.1.2 (Kearse et al., 2012). The contigs were queried against the online NCBI BLAST database to discard possible contamination.

Phylogenetic analyses

Because of the absence of indel mutations, alignments of the cox1 and h3 protein coding genes were trivial. The ribosomal genes were aligned using the online version of the program MAFFT v. 7 (Katoh et al., 2019, available at http://mafft.cbrc.jp). We tried different alignment strategies which yielded similar results, and selected the G-INS-I algorithm, with default values (0.53 gap penalty, 0.123 offset value) for final concatenation.

Topological incongruence between genes was examined by inferring individual gene trees using maximum likelihood as implemented in the IQ-TREE software v1.6.1 (Nguyen et al., 2015) under a generalized time-reversible model and 1000 replicates of ultrafast bootstrap (Thi Hoang et al., 2018) (Figs S1–S6). Since we did not find any significant incongruences, individual gene alignments were concatenated in a supermatrix with Geneious. Non-sequenced fragments were considered as missing data. The final matrix included 194 terminals and 6690 characters, with 48.18% missing data.

We assessed the impact of missing data on the results by analysing matrices with increasing levels of compactness. We used trimAL v1.2 (Capella-Gutiérrez et al., 2009) to generate matrices by removing columns with more than 75, 50 and 25% gaps, respectively. The best maximum likelihood tree for each matrix was inferred with IQtree (same settings as before). The results proved that removal of missing data had marginal or no effect either in the topology or on the support of the recovered clades (Figs S7–S10). Therefore, all subsequent analyses were conducted on the entire data matrix.

We conducted phylogenetic analyses under different inference methods (i.e. parsimony, maximum likelihood and Bayesian inference), to assess systematic error, i.e. the sensitivity of the results to changes in methodological assumptions (Wheeler, 1995; Ribeiro et al., 2012). Phylogeny reconstruction methods that incorporate explicit models of evolution (e.g. maximum likelihood) have been suggested to outperform non-parametric approaches (e.g. parsimony) (Huelsenbeck, 1998; Felsenstein, 2004; but see Siddall and Whiting, 1999; Pol and Siddall, 2001) because of their lesser sensitivity to the presence of long branches in non-related taxa, i.e. the long branch attraction artefact (Hendy, 1989). In recent years, the characterization of more realistic evolutionary properties of nucleotide sequences has sparked an ongoing debate on the relative performance and advantages of parsimony vs. maximum likelihood (Kolaczkowski and Thornton, 2004; Lockhart and Steel, 2005; Spencer et al., 2005; Thornton and Kolaczkowski, 2005; Lockhart et al., 2006; Simmons et al., 2006). Particularly controversial is the concept of "heterotachy", defined as the differences of evolutionary rates at specific sites among lineages because of changing selective constraints (Lopez et al., 2002). The relevance of heterotachy in the context of phylogenetic reconstruction is that current maximum likelihood implementations assume an identically distributed evolutionary process for all sequence sites. A recent simulation study suggested that parsimony can be better than standard likelihood at recovering the true tree given heterotachy (Kolaczkowski and Thornton, 2004), although the results and conclusions have been criticized on methodological and empirical grounds (Philippe et al., 2005; Spencer et al., 2005). The limitations of current inference methods advocate for a pluralistic approach, followed by a critical evaluation of the results obtained under parsimony and model-based analyses (Thornton and Kolaczkowski, 2005).

Parsimony analyses were conducted with TNT v1.5 (Goloboff and Catalano, 2016). We implemented a driven new technology search strategy consisting in the combination of sectorial searches, ratchet, drift and tree fusing, set to hit independently 10 times the minimum length. Support values were estimated by jackknifing frequencies derived from 1000 resampled matrices, using 10 random addition sequences, and retaining 10 trees per replication, followed by TBR (tree bisection and reconecction) and TBR collapsing to calculate the consensus. Parsimony analyses were conducted under two different gap scoring strategies. First, we analysed the complete matrix, considering the gaps as missing data. Second, we scored the gaps as additional presence/absence characters according to a set of rules based on gap overlapping and sharing of the 5′ and/or the 3′ termini (Simmons and Ochoterena, 2000). This coding implementation minimizes the effect of increasing the weight of overlapping multiple non-homologous gaps that results from scoring gaps as an additional state (Pons and Vogler, 2006). Automatic recording of the gaps was conducted with the program FastGap v1.2 (Borchsenius, 2009).

The best-fit partitioning scheme and nucleotide substitution models for model-based inference were selected with Partition Finder v2.1.1 (Lanfear et al., 2017). We predefined 10 partition blocks and six possible partition combination schemes (Table S5) and tested them based on the Bayesian information criterion. Preliminary trees were obtained with PhyML (Guindon et al., 2010) assuming linked branches. The best partition scheme consisted of 10 partitions (by gene and by codon position in protein coding sequences). Further information on partition scores and best-fit nucleotide evolution models are summarized in Tables S5 and S6.

Maximum likelihood analyses on the concatenated matrix were carried out with two different programs, IQtree v1.6.2 (Nguyen et al., 2015) and RAxML v8.2.10 (Stamatakis, 2014). The IQtree analysis was run under the preferred partition and evolutionary models, with 1000 replicates of complete non-parametric bootstrap and edge equal partition model (Chernomor et al., 2016). For the RaxML analysis, we defined the preferred partition scheme, but used the generalized time-reversible model instead. We accounted for heterogeneity with the CAT approximation, which integrates rate heterogeneity at a low computational cost (Stamatakis, 2006). The tree search strategy in RAxML consisted of 1000 iterations (distinct starting trees). Support values were estimated with multi-parametric bootstrapping and a random seed value of 12 345. Bootstrapping was halted automatically when it fulfilled the extended majority-rule consensus tree criterion (autoMRE), which ensures enough bootstrap replicates to recover stable support values.

Bayesian inference was implemented with MrBayes v3.2.6 (Ronquist and Huelsenbeck, 2003) under two different partition schemes, the best partition scheme (10 partitions) and a simplified partition scheme by gene (six partitions) (Tables S5 and S6). In both cases, the analysis consisted of two Markov Chain Monte Carlo runs of 50 million generations, sampling trees and parameters every 1000 generations. Each run included eight chains with a "heating temperature" of 0.15. We ensured that the Markov chains had reached

stationarity, and we examined the effective sample size values and the convergence of the independent run chains with the program TRACER v. 1.7 (Rambaut et al., 2018). The burn-in was set to the 25% first generations, after confirming in TRACER that it was enough to remove suboptimal generations. The posterior probability of the clades was used as a measure of support. All model-based analyses were run remotely on the CIPRES Science Gateway (Miller et al., 2010).

The obtained trees were visualized with FigTree v1.4.3 (Rambaut, 2009). To assess the sensitivity of the recovered clades to changes in the analytical procedure (i.e. inference methods, gap coding strategies and software), we selected the best resolved tree and mapped on it the support levels obtained for each clade with each of the methodologies.

Timetree estimation

We inferred a timeline for the diversification of Dysderidae and related outgroups within a Bayesian framework. Before running the analyses, and to reduce the branch length heterogeneity, we removed terminals with branch lengths over 0.25, as estimated in the consensus tree inferred in MrBayes with 10 partitions, unless they were the only representative of its family. Additionally, we removed short branches (<0.02), unless they involved calibration points (see below), under the assumption that they most likely represented coalescent relationships within species. Each coalescent clade was represented by the member with the greater number of sequenced genes.

Multiple calibrations are desirable when using relaxed-clock models because they help to identify the patterns of evolutionary rate variation among lineages (Ho and Phillips, 2009). Here, we combined calibration points based on both fossil data (seven, including root constraint) and biogeographic events (six) (see Table S7 and Figs S17 and S18). Fossil calibration points were mostly defined according to the revision on the fossil record of spiders by Magalhaes et al. (2020). The only exception was *Dasumiana emicans* Wunderlich, 2004, from Baltic amber, originally proposed as a crown Harpacteinae assuming its close relationship to extant genus *Dasumia* Thorell, 1875. However, our results ("Timetree estimation" section) suggests that *Dasumia* may not be monophyletic, and hence we used it as a minimum constraint for the stem Harpacteinae instead. We included fossil constraint information as prior log–normal distributions of the selected nodes. Because of the sparse fossil record of spiders, we used a hyperprior (uniform distribution) on the mean (M) of the log–normal prior distribution to avoid a false sense of accuracy on any specific number. Additionally, we constrained the root of the tree by defining a uniform prior ranging from 164 Ma—the minimum age of *Eoplectreurys gertschi* Selden & Huang, 2012 (Daohugou Beds, China), which has been interpreted as a stem Synspermiata (Magalhaes et al., 2020)—to 374 Ma (South Mountain, New York), the minimum age for the split of spiders (Araneae) from their sister extinct lineage Uraraneida (Selden et al., 2008).

We derived biogeographic information on time from two main sources, namely vicariant events and colonization of oceanic islands. We included two vicariant events, the Hercynian belt opening, dated at 33–25 Ma (Rosenbaum et al., 2002; Schettino and Turco, 2006), and the opening of the Strait of Gibraltar, dated at approximately 5.3 Ma. Previous studies have demonstrated that the split of the Iberian and the island species of the dysderid genus *Parachtes* Alicata, 1964 was most likely the result of the opening of the western Mediterranean Basin resulting from the Hercynian belt opening (Bidegaray-Batista and Arnedo, 2011). Therefore, we constrained a normal prior distribution on the corresponding node with mean 29 Ma and standard deviation 2.5. Similarly, the opening of the Strait of Gibraltar, following the Messinian Salinity Crisis, was assumed to have caused the split of the Iberian species *Dysdera inermis* Ferrández, 1984 and its sister species in Morocco. In this case we set a normal prior distribution to the corresponding node in the tree with mean 5.3 and standard deviation 0.5.

Regarding island colonization events, the chronological arrangement of islands in volcanic hot-spot archipelagos provides hard maximum bounds on divergence times for the lineages inhabiting the islands (Fleischer et al., 1998), assuming that the diversification was a consequence of the island colonization but may have occurred much later than the island formation (Ho and Phillips, 2009). The diversification of the genus *Dysdera* in the Canary Islands provides multiple examples of sister species, or populations, distributed on neighbouring islands (Macías-Hernández et al., 2008, 2016), which can be used as calibration points. Specifically, we used the age of La Palma (2 Ma) (Carracedo and Day, 2002) as a maximum bound for the split of the sister lineages within the species *D. silvatica* Schmidt, 1981 and *D. calderensis* Wunderlich, 1987 in La Gomera and La Palma. Similarly, the age of El Hierro (1.2 Ma) (Carracedo and Day, 2002) was established as a maximum bound for the split of the sister lineages of both *D. silvatica* and *D. gomerensis* Strand, 1911 in La Gomera and El Hierro. To account for the possibility of within-island divergences predating the colonization of the new island, as well as the possibility that colonization post-dated island emergence, we defined a normal prior distribution on the split of the corresponding island lineages, with the island age as mean and standard deviation 1 for La Palma and 0.5 for El Hierro (Table S6).

Since the use of geological events (Hipsley and Müller, 2014) and island age (Heads, 2011) for time estimation has been criticized, we conduct analyses with and without biogeographic information. Constrained nodes were forced to be monophyletic to ensure that prior distributions were correctly assigned and to speed up analyses. In all cases, the constrained nodes had already been shown to be supported in non-time-aware phylogenetic analyses, except for the sister group relationship of the Synspermiata and the Hypochilidae + Filistatidae lineage, which was not supported in our analyses but has been systematically recovered and supported in phylogenomic analyses (Garrison et al., 2016) and in analyses with more extensive taxonomic sampling (Wheeler et al., 2017).

Time divergence estimation analyses were conducted under a Bayesian uncorrelated relaxed molecular clock approach as implemented in BEAST v2.6.3 (Bouckaert et al., 2019). To facilitate correct mixing and chain convergence, we reduced the number of parameters by defining a partition by gene (six partitions) instead of the preferred 10 partition scheme (Table S8). The best-fit models selected by Partitionfinder for each partition are given in Table S9. The best tree prior and clock for each individual gene were selected using Bayes factors, estimated by means of Path and Stepping Stone sampling (Baele et al., 2013) (Table S9). We generated a starting tree including time constraints with the program PATHd8 (Britton et al., 2007).

Preliminary analyses were conducted to cross-validate the multiple calibration points included and to fine tune the different parameters. These analyses consisted of single chain runs of 50 million generations, sampling every 10 000 generations. For the final analyses, three independent chains were run under selected priors for 100 million generations, sampling every 10 000 generations. Convergence among runs and correct mixing of the chains was monitored with TRACER v.1.7 (Rambaut et al., 2018). In the analyses that included biogeographic calibrations, the first 15% of generations from each chain were removed as burn-in. For analyses without biogeographic information the burn-in was set to 10, 10 and 30% of generations respectively. Finally, runs were combined with the help of the BEAST accompanying programs LOGCOMBINER and TREEANNOTATOR.

Diversification rates

We investigated shifts in diversification rates within the family in a Bayesian framework using the computer program BAMM

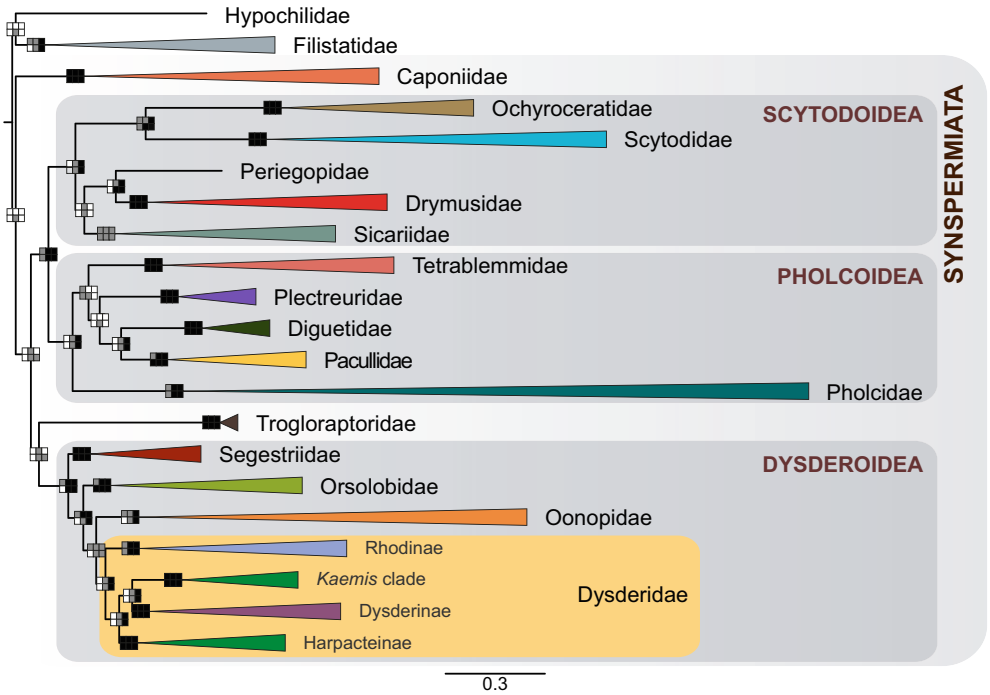

Fig. 3. Summary phylogenetic tree from concatenated analyses. RAxML maximum likelihood tree summarizing parsimony, maximum likelihood and Bayesian inference supports. Clade supports indicated in each node. Black square, supported by parsimony jackknife and maximum likelihood bootstrap >80%, or posterior probability >0.95; grey square, clade recovered but support <80% or 0.95 respectively; white squares, clade not recovered. Left column, parsimony, gaps as missing data (above), gaps as absence/presence (below); central column, maximum likelihood, IQtree (above), RAxML (below); right column, Bayesian inference, six partitions (above), 10 partitions (below).

(Rabosky, 2014; Rabosky et al., 2017) and the R package BAMMtools (Rabosky et al., 2014). We accounted for undersampling by estimating the proportion of species represented in the analyses out of the total species known in each genus (sampling fraction). In the case of genera that were recovered as non-monphyletic, we assigned non-sampled currently accepted species (World Spider Catalog, 2023) to the identified clades based on morphological traits. Our current knowledge of dysderid taxonomy is far from complete, and many new species await formal description. For each genus/clade, we did correct the total number of species by adding species that we are aware are awaiting formal description, based either on our own knowledge or from personal communication from collaborators (Table S11). We assessed the impact of prior parameterization on our results by conducting analyses under different priors for the number of expected shifts (expectedNumberofShifts = 0.1; 1; 5; 10).

Results

The final dataset consisted of 220 specimens representing 18 families, 16 of them belonging to the Synspermiata clade, plus Hypochilidae and Filistatidae, which were included to root the trees. The family Dysderidae was exhaustively sampled, including 115 specimens representing at least 66 species and 23 out of the 25 recognized genera. The final data matrix consisted of 194 terminals. To maximize matrix occupancy, we combined sequences of different specimens into 22 single chimeric terminals (see Table S1). After concatenation, we obtained 6690 characters (cox1 = 1076 bp, 16s = 558 aligned positions, 18s = 1785 aligned positions, 28s = 2562 aligned positions, h3 = 328 bp, 12 s = 381 aligned positions) (Table S4). About 48% of the entries were missing data.

Phylogenetic inference

The trees inferred with the different analytical procedures were topologically highly congruent. We used the maximum likelihood tree topology obtained with RAxML to summarize the support values obtained in all of the analyses (Figs 3–6). Trees from each analysis are available as supplementary material (Figs S11–S16).

In general, posterior probabilities provided higher support values, followed by the maximum likelihood bootstrap and the parsimony jackknife. Overall, parsimony trees were less resolved, particularly at the higher taxonomic levels, but in agreement with the other methods. The topology and supports in the parsimony trees obtained with the gaps as missing data and the gaps scored as absence/presence did not differ significantly, and hence the model-based analyses were conducted with the gaps as missing data only.

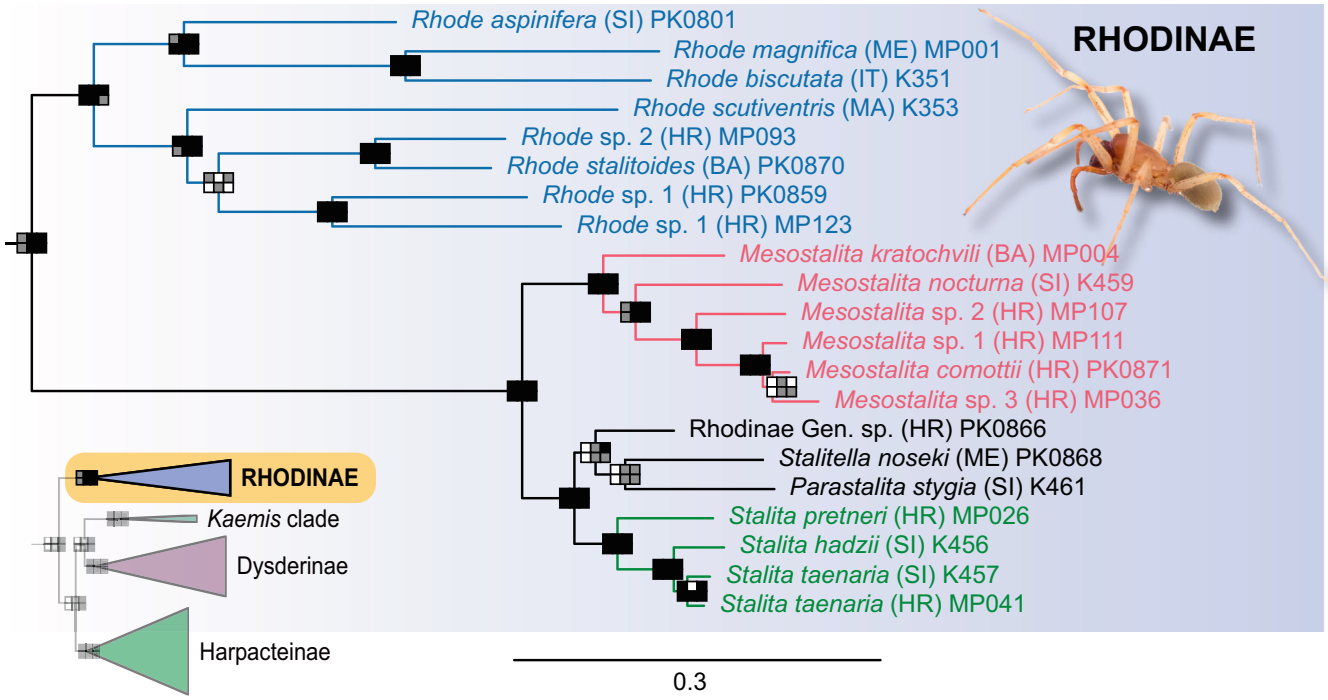

Fig. 4. Detail of the subfamily Rhodinae as recovered in Fig. 3. Supports coded as in Fig. 3. Species names coloured by genus. Terminals in black are either species represented by a single specimen or unidentified. Photo: *Stalita pretneri* (Rhodinae), credit Tin Rožman.

The model-based analyses recovered monophyly of all of the included families, most of them supported. However, interfamily relationships were poorly resolved. The superfamilies Dysderoidea, Scytodoidea and Pholcoidea were recovered in model-based approaches and supported in Bayesian analyses. Parsimony analyses, on the other hand, failed to recover the monophyly of Dysderidae, and also Filistatidae and Oonopidae in the case of the "absence/presence" coding. The position of Caponiidae and Trogloraptoridae was conflicting across analyses, yet poorly supported. Caponiidae was never recovered as sister to Dysderoidea, as found in recent phylogenomic analyses (e.g. Kallal et al., 2021; Kulkarni et al., 2021), and its unstable position was responsible for the paraphyly of Synspermiata, recovered in most analyses albeit with low support. Our analyses recovered, albeit with low support with parsimony, the sister group relationship of Scytodoidea and Pholcoidea. Interestingly, branches in Pholcidae, C. L. Koch, 1850 and, to a lesser extent, Scytodidae Blackwall, 1864 and Oonopidae, were all longer than the average, suggesting an acceleration of the substitution rates in these lineages.

In all analyses, except parsimony with gaps recoded, the world-wide distributed family Oonopidae was recovered sister to Dysderidae, albeit with low support. Within the family Dysderidae (Figs 4–6), the different analytical procedures generally converged in similar topologies. The subfamilies Rhodinae and Dysderinae were recovered as monophyletic and supported in most of the analyses. Conversely, Harpacteinae was not recovered as monophyletic in any of the analyses, mostly owing to the unstable position of a supported clade (*Kaemis* clade henceforth) formed by the genus *Kaemis* Deeleman-Reinhold, 1993, and the monotypic cave-dwelling genera *Sardostalita* Gasparo, 1999 and *Speleoharpactea* Ribera, 1982. The *Kaemis* clade was recovered as sister to Dysderinae in the model-based analyses, a relationship supported by Bayesian inference. The remaining Harpacteinae formed a supported clade (Harpacteinae henceforth), recovered as sister to the Dysderinae + the *Kaemis* clade, albeit with low support except in the Bayesian analyses.

All genera within Rhodinae and Dysderinae (Figs 4 and 5) were recovered as monophyletic. Conversely, most genera within Harpacteinae (Fig. 6) did not form monophyletic groups. Specifically, the genus *Folkia* Kratochvíl, 1970 was split into three distantly related lineages, and the representatives of *Harpactea* and *Dasumia* were intermingled within the clade.

Timetree estimation

After removal of too long and too short branches, the final data matrix for the dating analyses consisted of 157 terminals, 97 of them belonging to Dysderidae. The Bayes factor comparisons yielded strong evidence

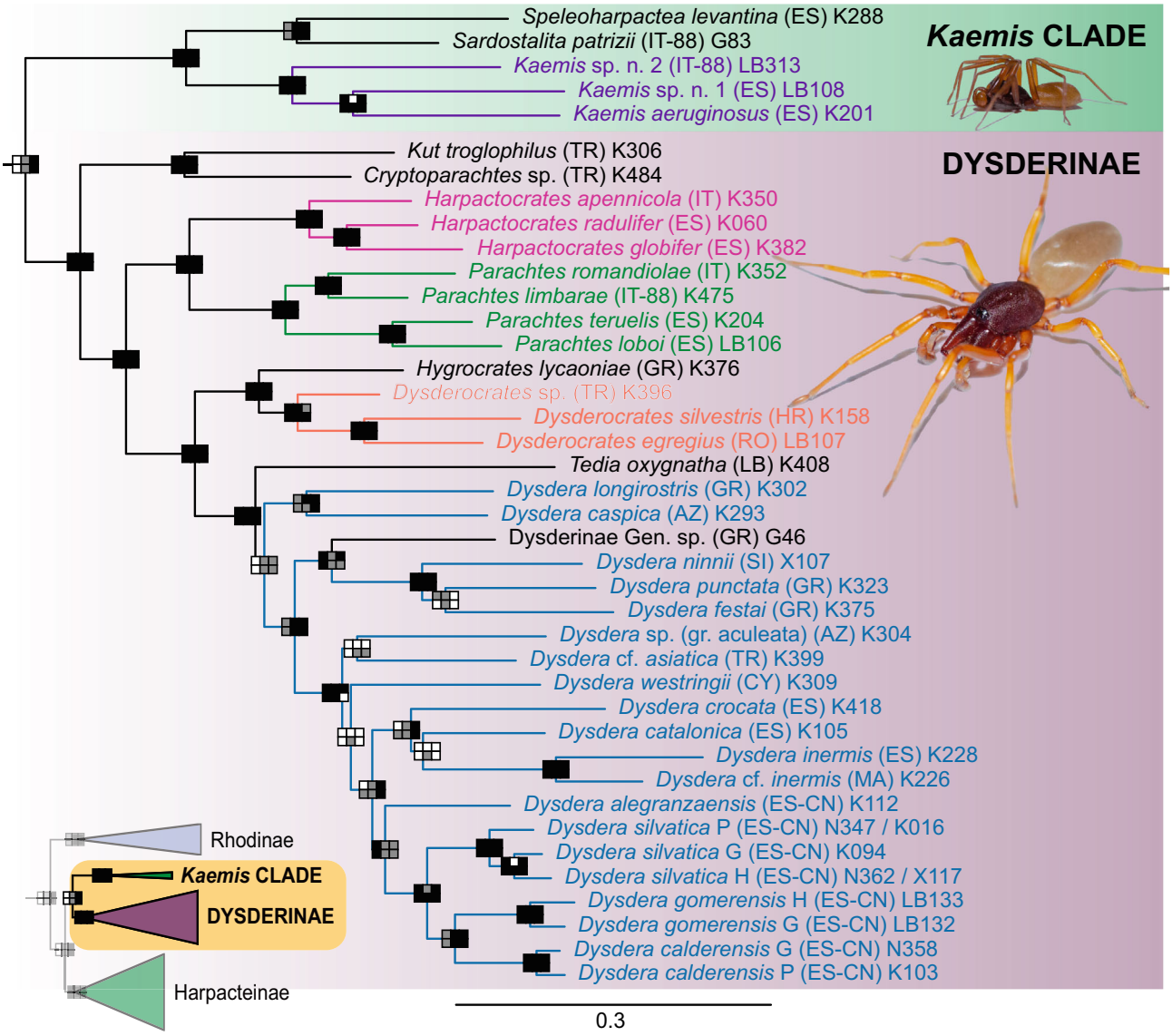

Fig. 5. Detail of the subfamily Dysderinae and the *Kaemis* clade as recovered in Fig. 3. Supports coded as in Fig. 3. Species names coloured by genus. Terminals in black are either species represented by a single specimen or unidentified. Photos: *Kaemis paitidarum* (*Kaemis* clade, above), credit Marc Domènech Andreu; and *Dysdera portsensis* (Dysderidae, bellow), credit Marc Domènech Andreu.

for the use of the Birth–Death tree and the relaxed log–normal clock priors, under both the path and the stepping-stone sampling (Table S10).

The results of the Bayesian tree dating inference are summarized in Fig. 7. Comparison between results of the analysis conducted using all calibration points and only those referred to fossils (Figs S17–S19) revealed a consistent pattern of slightly older ages (approximately 10 Ma in average) in the second, although confidence values largely overlapped. These differences were also reflected in the estimated substitution rates (ucdl.mean parameter) of the mitochondrial genes, which were higher in the analyses with all calibrations—0.011 (0.008–0.013), 0.006 (0.005–0.007), 0.006 (0.005–0.007) for cox1, 16s and 12s, respectively—than in the analyses with fossil calibrations only—0.009 (0.007), 0.005 (0.004–0.0055) and 0.005 (0.004–0.006). Differences in the rates of the nuclear genes, on the other hand, were hardly noticeable. Since estimates of the substitution rates with all calibration points are closer to estimates available in the literature from former studies, and they are more in agreement with independent evidence for the origin of some land masses (e.g. the Canaries), we will further discuss the results of analyses with all calibrations only.

The topology of the dating tree mostly mirrored the results of the non-time-constrained Bayesian phylogenetic analyses. The Dysderidae split from its sister group, the Oonopidae, at 121.1 Ma (95% confidence interval 132.3–110.2 Ma) and its extant diversity was

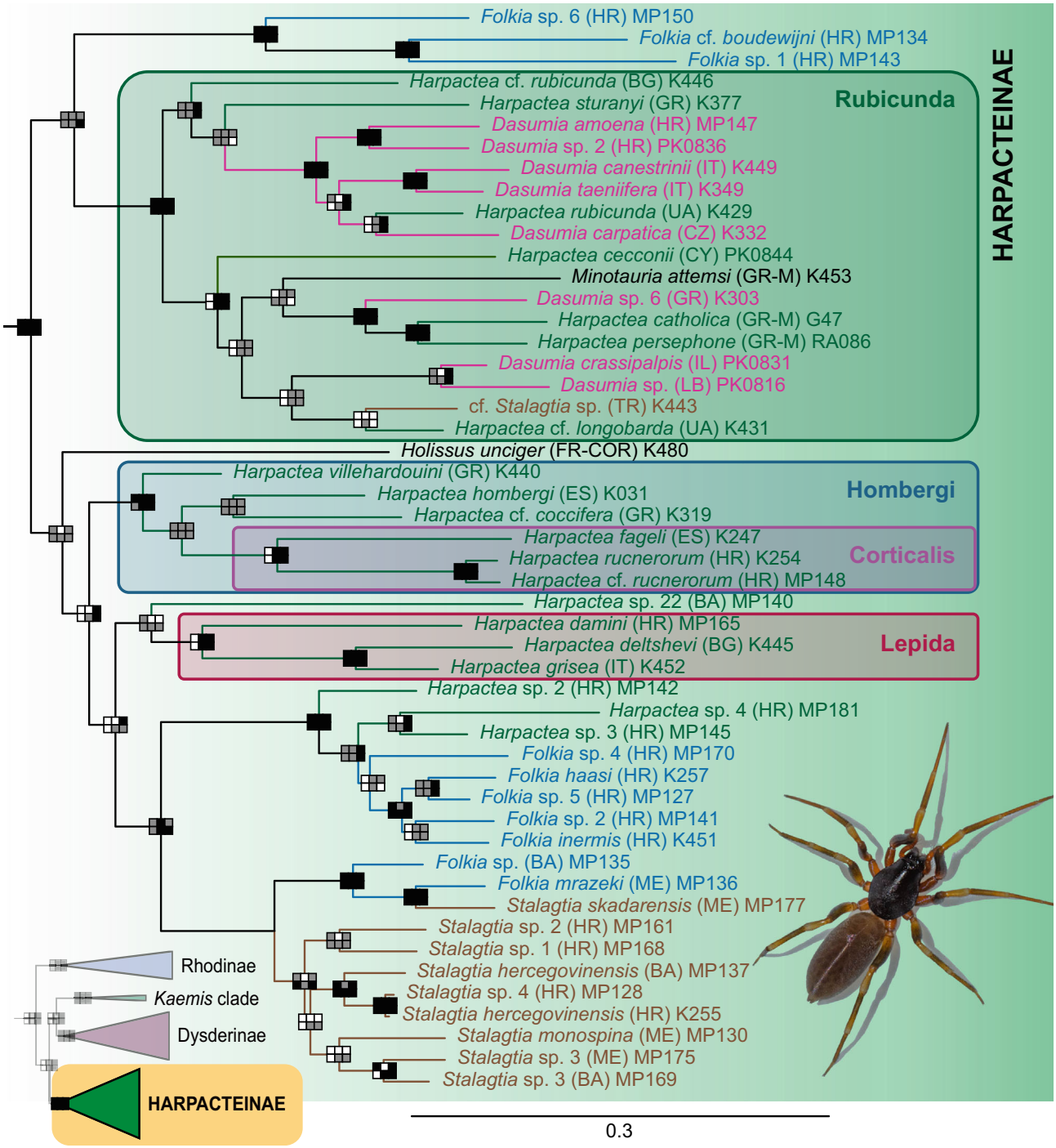

Fig. 6. Detail of the Harpacteinae clade as recovered in Fig. 3. Supports coded as in Fig. 3. Species names coloured by genus. Terminals in black are either species represented by a single specimen or unidentified. Photo: *Harpactea hombergi* (Harpacteinae), credit Marc Domènech Andreu.

traced back to 112.1 Ma (124.2–99.9 Ma), both during the Early Cretaceous. The diversification of its four main lineages started at a similar time window, during the Late Cretaceous: 88 Ma (101.5–73.7 Ma) for the Rhodinae, 77.5 Ma (88–67 Ma) for the Dysderinae, 76.9 Ma (88.7–66) for the Harpacteinae and 68 Ma (82.6–54 Ma) for the *Kaemis* clade.

Interestingly, some lineages formed mostly by cave-adapted species had long stem branches, dating back to the Palaeocene or earlier, but they did not start

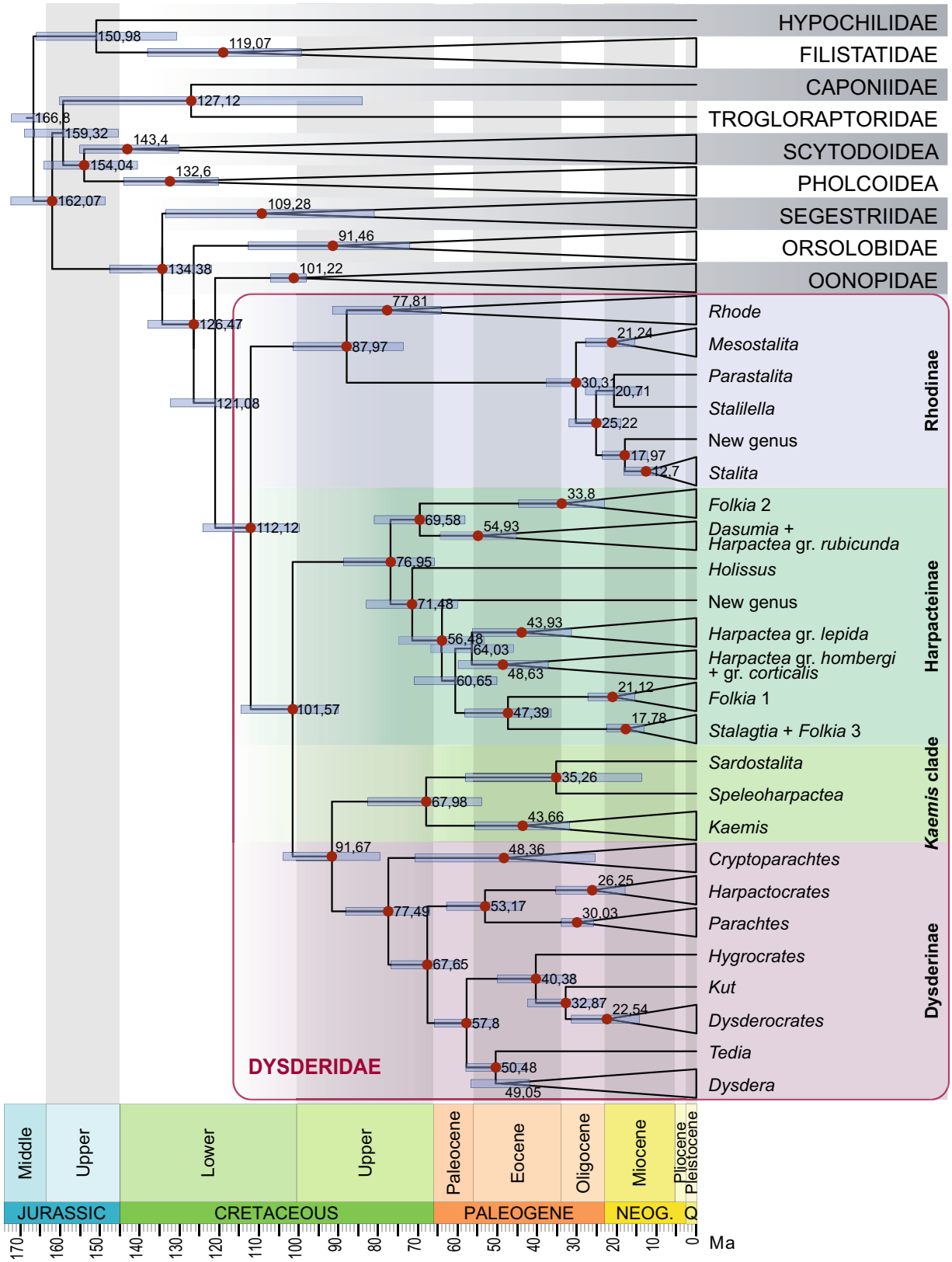

Fig. 7. Chronogram inferred with BEAST. Node labels correspond to the estimated age. Bars on nodes show the 95% confidence intervals on the node age. Red circles correspond to supported nodes (posterior probability >0.95). Collapsed groups within Dysderidae correspond to nominal genera in the case of Dysderinae, Rhodinae and *Kaemis* clade, and to species groups as coded for the BAMM diversification analyses for Harpacteinae.

diversifying until the Early Oligocene. Specifically, the Rhodinae lineage including *Mesostalita* Deeleman-Reinhold, 1993, *Parastalita* Absolon & Kratochvíl, 1932, *Stalita* Schiödte, 1847 and *Stalitella* Absolon & Kratochvíl, 1932 split from *Rhode* Simon, 1882 at 88 Ma (101.5–73.7 Ma), although extant diversity in the group was much more modern, and dated back to 30.3 Ma (37.8–23.7 Ma). Similarly, the *Folkia* lineages split from its closest relatives at 60.6 Ma (71–50.1 Ma) and 69.6 Ma (81–58.2 Ma), respectively, but did not start diversifying until 21.1 Ma (27.3–15.5 Ma), 17.8 (22.5–13.1 Ma) and 33.8 Ma (44.7–23.1 Ma), respectively. Other relevant estimates involved the cave-dwellers *Sardostalita patrizii* (Roewer, 1956) from Sardinia and the northeastern Iberian *Speleoharpactea levantina* Ribera, 1982, which split at 35.3 Ma (58.1–13.7 Ma).

Diversification rates

The use of alternative priors on the number of rate shifts had little effect on the results, suggesting that the analyses were robust to prior influence. Therefore, we only report the results obtained with prior rate shift of 1, summarized in Tables S12–S14. BAMM identified up to five rate shifts, although the three with the highest posterior probability accounted for almost 80% of the probability. Bayes factors indicated strong evidence for a shift in diversification dynamics somewhere near the origin of *Dysdera* (Fig. 8). The configuration with the highest probability indicated a shift along the branch leading to *Dysdera* with the exclusion of the first offshoot within the genus, encompassing *D. adriatica* Kulczyński, 1897 and *D. caspica* (posterior distribution = 0.68). The second shift was assigned along the branch leading to the last common ancestor of *Tedia* Simon, 1882 and *Dysdera* (0.21), and the third to the branch leading to *Dysdera* (0.06). The estimated speciation rates in the nodes with shifting rates (lowest 0.13, quartiles = 0.07–0.021) were more than twice the overall tree rate (0.06, 0.05–0.08).

DISCUSSION

Origin and diversification of Dysderidae

Because of their conservative morphology and ecology, the monophyly of Dysderidae has never been seriously questioned. Surprisingly, some of our analyses either did not recover (parsimony) or yielded low support (maximum likelihood) for the family's monophyly. Oonopidae was the closest Dysderidae relative in all our analyses, albeit with low support, and the few instances of non-monophyly were due to the inclusion of this family within the Dysderidae (Fig. 3; Figs S11–S16). However, most previous studies have either recovered (Wheeler et al., 2017) or unambiguously supported (Fernández et al., 2018; Michalik et al., 2019; Kulkarni et al., 2021; Ramírez et al., 2021) the Gondwanic family Orsolobidae as sister to Dysderidae. The long branches of the oonopids observed in our trees may hint at an artefactual position owing to a long branch attraction effect (Bergsten, 2005). Although most of the outgroup sequences used in our study come from Wheeler et al. (2017), the sparser taxonomic sampling across outgroups in our study may have exacerbated the branch length dissimilarity. It is interesting to note that a previous study on false violin spiders (Synspermiata: Drymusidae Simon, 1889) using similar markers and outgroup sampling also recovered Oonopidae as sister to Dysderidae (Labarque et al., 2018).

Our time estimates traced the origin of the Dysderidae back to the Early Cretaceous, approximately 120 Ma (95% confidence interval 132.3–110.2 Ma) (Fig. 7). Interestingly, these estimates match the time of formation of the Tethys Sea, which marked the complete separation of Gondwana from Laurasia, approximately 120–100 Ma (McIntyre et al., 2017). If the sisterhood between the Gondwanic Orsolobidae and the Laurasian Dysderidae, supported in multiple phylogenomic analyses, holds, our time estimates will point towards the involvement of the continental split in the origin of Dysderidae. On the other hand, tectonic and palaeogeographic–palaeoenvironmental reconstructions indicate that during the Late Cretaceous (100.5–66 Ma), a shallow epicontinental sea dotted with variously sized islands covered most of what is now Europe (Seton et al., 2009; Csiki-Sava et al., 2015). The isolation or colonization of the primary land masses within this Cretaceous archipelago offers an alternative plausible explanation for the family's origin, characterized by its relatively constrained distribution, predominantly confined to the circum-Mediterranean region, despite its remarkable species richness. Additionally, these factors probably contributed to the divergence of its major lineages. Our results suggest a substantial temporal overlap with the divergence of Dysderidae subfamilies, with a time window of 120–80 Ma.

It is important to note that one of our calibration points depends on the monophyly of the Onychoceratidae family. This family was found in the most up-to-date spider phylogeny, in terms of markers and taxonomic sampling, albeit with low support (Kulkarni et al., 2023). However, this finding has been challenged by recent total evidence analyses of the Scytodoidea superfamily (Magalhaes et al., 2022).

Overall, our phylogenetic analyses supported current subfamily divisions of dysderids, except for Harpacteinae that was resolved as paraphyletic regarding

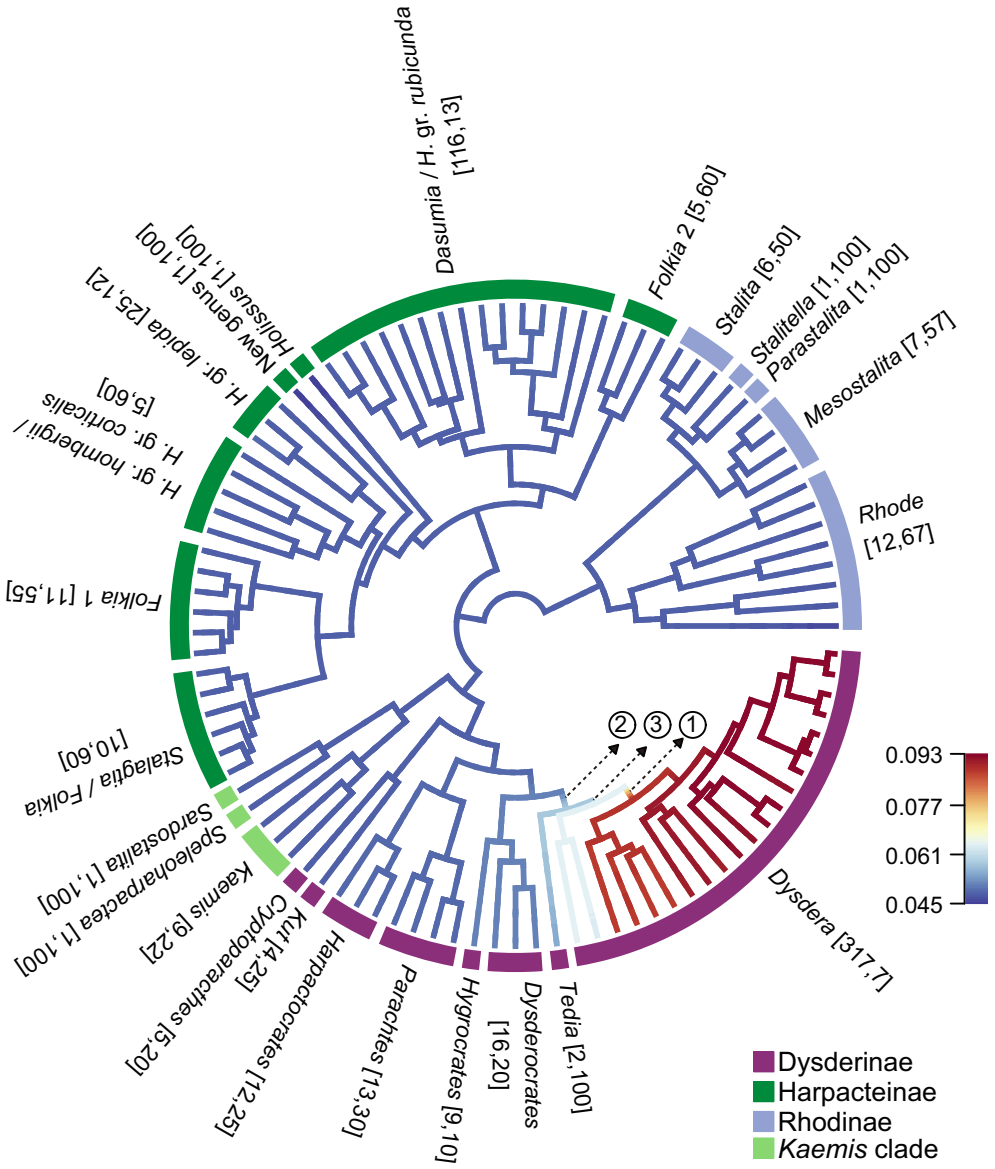

Fig. 8. BAMM plot. Phylorate plot with the most frequent shift configuration identified with BAMM. Branch colours indicate model averaged diversification rates. Numbers on nodes identify the three configuration shifts with highest BF compared with no shifts (>10). Labels on tips indicate genus/clades. Numbers in square brackets on labels refer to the estimated number of species per genus/clade and the percentage of its diversity sampled in the study (see Tables S12–S14).

Dysderinae. These results were already advanced by Platania et al. (2020), although with a sparser taxonomic sampling. Although never explicitly tested, the shared presence of a long labial margin of the sternum suggested that Rhodinae and Dysderinae were more closely related (Deeleman-Reinhold and Deeleman, 1988), which stand at odds with our results. Our analyses split Harpacteinae into two well-supported clades, one including the bulk of the genera and a second one, closer to Dysderinae (the *Kaemis* clade), encompassing the two cave-dwelling monotypic genera *Sardostalita* and *Speleoharpactea*, and the mostly edaphic genus *Kaemis* (Figs 5 and 6). The last genera were originally included in Harpacteinae owing to the trapezoidal frontal margin of the sternum and the absence of claw tufts. However, they share some traits that differ from the rest of Harpacteinae and support their monophyly, such as spineless legs, barrel-like male palpal tegulum, and large and long posterior diverticle of the vulva. Nevertheless, there are no evident morphological synapomorphies to support its closest relationship to Dysderinae. Based on current knowledge we suggest that the *Kaemis* clade could constitute a fourth subfamily within

Dysderidae, but that will be dealt with in further research.

Additional characters are needed to support subfamily relationships and reject Harpacteinae monophyly, as only model-based approaches recovered the sister group relationships among Dysderinae, the *Kaemis* clade and Harpacteinae.

An unexpected lineage

Interestingly, the *Kaemis* clade lineage (Fig. 5) includes both cave-dwellers and edaphic species, some of which have been found in deep pitfall traps in the mesovoid shallow substratum. This highlights the possible role of the mesovoid shallow substratum as a stepping-stone stage towards cave adaptation (White and Culver, 2007). The closer relationship recovered between *Spleoharpactea* and *Sardostalita* is supported by their cheliceral teeth. Both bear three teeth on the promargin and one basal tooth on the retromargin, while *Kaemis* has two on the promargin and two on the retromargin, the same condition as observed in Harpacteinae. *Sardostalita patrizii* is endemic to Sardinia and *Speleoharpactea levantina* is found in the karstic region between northern Valencia and southern Catalonia, in the northeastern Iberian Peninsula. Interestingly, before the early Oligocene (30 Ma), these areas were part of a continuous block called "Greater Iberia", but subsequently fragmented and separated during the opening of the Western Mediterranean Basin (Siravo et al., 2023). Our timeline estimates are fully congruent with these geological events (time of split 35.3, 58.1–13.7 Ma), providing additional evidence of the relevance of tectonic events for the diversification of Mediterranean biota (Bidegaray-Batista and Arnedo, 2011).

A taxonomic nightmare

Our results indicate a state of taxonomic confusion in the core lineage of Harpacteinae, with almost all genera found to be non-monophyletic (Fig. 6). These results were largely expected, since several authors had already acknowledged the rather poor definition of the Harpacteinae genera (Chatzaki and Arnedo, 2006; Deltshev, 2011). It has long been accepted that *Harpactea* was not a natural group, but rather a generalized form from which more specialized lineages evolved (Deeleman-Reinhold, 1993). The recent molecular analysis in Platania et al. (2020) already corroborated these observations, confirming the polyphyly of *Harpactea*. Several species groups have been proposed in the literature to further classify *Harpactea* species owing to their heterogeneity (Alicata, 1966; Brignoli, 1978; Deeleman-Reinhold, 1993). Deeleman-Reinhold's classification (1993) has been mostly adopted by subsequent authors, either describing new species or completing former descriptions. It includes four groups, namely corticalis, hombergi, lepida and rubicunda, defined by female vulva traits, which were more reliable than the male bulb traits used in Alicata's and Brignoli's proposal (although some groups partially overlap). Some authors have already proposed to elevate these groups to the genus level (Deltshev, 2011). Mapping species groups onto our phylogenetic trees would partially support their generic status (Fig. 6). The rubicunda group would also include the nominal species of *Dasumia* and *Minotauria* Kulczyński, 1903. Deeleman-Reinhold (1993) already recognized the blurred limits between *Dasumia* and the rubicunda group, and suggested the inclusion in the group of the epigean *Stalagtia* Kratochvíl, 1970 from the Aegean and Anatolia, represented and confirmed in our analysis by cf. *Stalagtia* sp. (TR). The lepida group was recovered as monophyletic, supporting the results of Platania et al. (2020), which included a larger sampling of this particular group. Finally, the corticalis group rendered the hombergi group as paraphyletic. It should be borne in mind, however, there are still numerous lineages that would not fit into this classification.

The genus *Folkia* was also split into different lineages in our analysis. The first clade would probably include the nominal species *Folkia boudewijni* Deeleman-Reinhold, 1993, and was recovered as more closely related to the rubicunda group + *Dasumia* + *Minotauria* clade. A second clade, encompassing the type species *Folkia inermis* (Absolon & Kratochvíl, 1933) and the nominal species *Folkia haasi* (Reimoser, 1929), was recovered in all analyses as sister to a clade that included the species *Folkia mrazeki* (Nosek, 1904), but also all *Stalagtia* species from the Dinarides, including the type species *Stalagtia hercegovinensis* (Nosek, 1905). Both the structure of the male palp and the geographic distribution seem to support these three distinct lineages: the lineage including the type species of *Folkia* is mostly distributed in middle and south Dalmatian islands and nearby continental land, the lineage including *F. boudewijni* and relatives would be found near the coast and on Dalmatian islands circumscribing the former localities, and the lineage including *F. mrazeki* is found deeper in the continent and to the south, in Bosnia and Herzegovina and in Montenegro.

A definitive redefinition of the Harpacteinae at generic levels falls outside the limits of the present study. This will have to wait for a more exhaustive species sampling and a careful evaluation of the morphological traits. If morphological criteria alone fail to univocally delimit generic groups, an interesting alternative would be to explore the use of taxa age limits, as has been proposed in taxonomically challenging butterfly groups (Talavera et al., 2013).

The dark side of the red devils

Rhodinae monophyly was supported by all the analyses (Fig. 4). Its internal structure was well resolved, with all its genera recovered as monophyletic. With 18 species (World Spider Catalog, 2023), Rhodinae is relatively species poor compared with the other Dysderidae subfamilies. Its main centre of diversification seems to lie in the Dinarides, where four out of the five known genera and most of the species are localized. Only *Rhode* has been reported outside the region, with species in Corsica, the Iberian Peninsula, northern Africa, and Italy.

The classification of non-*Rhode* dinarid cave-dwelling species into four different genera (Deeleman-Reinhold and Deeleman, 1988) has been questioned by several authors based on their close phenotypic resemblance. Our results recovered the monophyly of the two non-monotypic genera. Nevertheless, they also revealed that their divergence times are much younger than those observed among most of the currently recognized genera within the family (Fig. 7), providing further support for the synonymy of all four genera under a single genus, *Stalita*.

Rhodinae holds a great evolutionary interest for the study of cave evolution, since four of its genera (*Mesostalita*, *Parastalita*, *Stalita* and *Stalitella*) are exclusively troglobiotic, and the fifth (*Rhode*) also includes cave-dwelling species, all of which are distributed in the Dinaric Alps. The stem of the troglobiotic clade is much longer that the one observed in *Rhode*, and one of the largest branches in the red devil spider tree. A long branch may be indicative of recurrent extinction events within the lineage, as proposed, for example, to explain the restricted distribution of the dysderini genus *Harpactocrates* in western European mountain ranges (Bidegaray-Batista et al., 2014). Our estimated timeline suggests that the extant *Stalita*-like species, including all Rhodinae genera but *Rhode*, would be the descendants of a single lineage that survived the Eocene–Oligocene Transition, which occurred about 33.9 Ma. This period was crucial in the history of the Earth because it was a time when the climate began to resemble the modern 'icehouse' climate with the formation of large ice sheets in Antarctica. This led to significant changes in ocean circulation and global climate. As a result, there were also major turnovers in marine and terrestrial biotas (Prothero and Berggren, 1992). Subsequent episodes of general cooling and a decrease in precipitation, such as those recorded during the Middle Miocene Climatic Transition (~14 Ma) in southern Europe (Botsyun et al., 2022), could have driven surviving lineages to find refuge in the underground environment in search of more humid and stable conditions (Mammola et al., 2015; Ballarin and Li, 2018). It is worth highlighting that similar crown ages were also inferred for the two strictly cave-dwelling clades in the subfamily Harpacteinae, namely *Folkia* and *Folkia* + *Stalagtia*, which would provide further support for this scenario.

The success of specialization

Our results provide univocal support for the monophyly of the subfamily Dysderinae (Fig. 5). The results support the replacement of the middle claw by hair tufts (scopulae) in all legs as a synapomorphy of the subfamily (the Harpacteinae genus *Dasumia* also bears claw tufts but only in posterior legs). Unlike Harpacteinae, internal relationships within Dysderinae were congruent with the current taxonomic classification. Our results mirrored those found in previous studies (Bidegaray-Batista and Arnedo, 2011; Bidegaray-Batista et al., 2014) regarding topology. However, our time estimates were older, yet with overlapping confidence intervals (Fig. 7). Upon comparison, we found an error in former molecular analyses owing to mislabelling: *Dysderocrates* sp. (TR) and *Kut troglophilus* were mispositioned. The sister group relationships of *Cryptoparachtes* and *Kut* is further supported by the similar structure of the vulva of these two genera. We found support for *Tedia* as the closest relative to *Dysdera* across all analyses. *Tedia* strongly resembles *Dysdera* in both somatic morphology and female genitalia. The differences between the two genera are restricted to the male bulb, which has an extremely reduced (or absent) distal haemathodocha in *Tedia*. In the closest related genera *Dysderocrates* Deeleman-Reinhold and Deeleman, 1988 and *Hygrocrates* Deeleman-Reinhold and Deeleman, 1988, the distal haemathodocha is also poorly developed. Consequently, the presence of a well-developed distal haemathodoca could be considered a synapomorphy of *Dysdera*. It should be borne in mind, however, that the monophyly of *Dysdera* is recovered, but not supported in any of the analyses. Additional data would be required to confirm the reciprocal monophyly of *Tedia* and *Dysdera*, or otherwise to synonymize the two genera.

Our results confirmed that the remarkable species richness observed in *Dysdera* is not a taxonomic artefact. Indeed, the results of the BAMM analyses identified an increase in diversification rates at the base of *Dysdera* (Fig. 8). Conversely, after correcting for taxonomic inconsistencies, the same was not observed in *Harpactea*, the other remarkable species-rich genus in the family. However, the results of the BAMM analyses should be taken with a pinch of salt, owing to the sparse taxonomic sampling. In some cases, fewer than 10% of the species were sampled, and many

species were assigned to the clades identified in our phylogenetic analyses on an ad hoc basis. Additionally, several recent studies have expressed some concerns on the validity of the results of BAMM analyses (Moore et al., 2016; Meyer et al., 2018). While some of the criticisms have been shown to be unfounded (Rabosky et al., 2017), a certain caution should be exerted with regards to the strength of our results.

The evolutionary success of *Dysdera*, in terms of number of species, is probably due to multiple factors that are yet to be quantitatively tested. While the investigation of the importance of those factors is beyond the scope of the present paper, we will take the opportunity to propose some hypotheses that could be interesting to test in further research.

Trait variation has been proposed to drive more tightly packed distribution and ultimately morespecies-rich communities, by preventing competition with neighbouring species (Barabás et al., 2022). One of the most evident morphological traits, distinguishing *Dysdera* from any other dysderid genera (except *Parastalita*), is the presence of protruding chelicerae. Moreover, across the genus, the size and shape of the chelicerae vary, which is unusual for spiders, which are usually conservative in these traits within genera. These cheliceral modifications have been related to a shift in dietary preferences to specialize in feeding on woodlice (onychophagy) (Arnedo et al., 2007; Řezáč et al., 2021; Bellvert et al., 2023), a prey usually rejected by most predators (Pekár et al., 2016). Similar adaptations have also been observed at the metabolic, physiological and genetic level (Hopkin and Martin, 1985; Toft and Macías-Hernández, 2017; Vizueta et al., 2019). The coexistence of different predatory strategies could explain the remarkably high levels of species co-occurrence reported in *Dysdera*.

Although less important, another potential driver of diversification in *Dysdera* is ecological shifts. Dysderids are generally very conservative in terms of ecology and habitat preferences. The major exception across the family is adaptation to the underground environment that, as discussed above, is prevalent in some of the main evolutionary lineages. There are also examples of cave-adapted *Dysdera* (Deltshev, 1999; Arnedo et al., 2007). Moreover, *Dysdera* is exceptional within Dysderidae in the existence of species adapted to the intertidal environment (Deeleman-Reinhold and Deeleman, 1988; Macías-Hernández et al., 2010).

Finally, the holokinetic structure of *Dysdera* chromosomes (Král et al., 2006) may have further contributed to *Dysdera* diversification. A recent study on the *Dysdera erythrina* species complex (Řezáč et al., 2018) revealed that closely related species differ in karyotype number and exhibit chromosome fusions, fissions and translocations. This observation suggested that chromosome rearrangements generating reproductive incompatibility may have played a primary role in speciation within *Dysdera* (Řezáč et al., 2018).

Conclusions

Dysderidae is a well-suited model system for studying diverse evolutionary questions. Nevertheless, its internal phylogenetic structure has yet to receive much attention. We have aimed to overcome this limitation by conducting a concatenated targeted gene phylogenetic and time divergence analysis of an extensive taxonomic sample within Dysderidae, complete at the genus level, and related families. The family originated and diversified in the Early to Middle Cretaceous, presumably favoured by isolation following the split of Pangea and the subsequent establishment of an island archipelago in present-day Europe. Our results identified four main evolutionary lineages: the already well-established Rhodinae and Dysderinae subfamilies, and two well-supported clades derived from the paraphyly of Harpacteinae. Additionally, we unveiled a great deal of taxonomical incongruence within the subfamily Harpacteinae, which needs a profound revision of the generic diagnostic traits to adapt its taxonomic classification to the actual phylogeny.

Our results support a significant increase in diversification rates at the base of the genus *Dysdera*. The unique presence in this genus of interspecific variability in mouthpart morphology, which has been linked to dietary specialization (Řezáč et al., 2008; Bellvert et al., 2023), could be identified as a potential driver. Further quantitative tests will be required to test this hypothesis. Conversely, the internal structure of *Harpactea* suggests that its diversity is an artefact derived from a poor definition of the genus.

Finally, the prevalence of cave adaptation within the family results from the combination of adaptive behaviours and long-term climatic changes, while time estimates of island colonization events are compatible with Mediterranean geochronology.

Acknowledgements

This study has been a long trip. We are in debt to all those colleagues and collaborators who helped us to gather all the specimens used in the study: J. Bedek, K. Cindrić, E. De Mas, M. Drčelić, F. Gasparo, GIET, G. Giribet, D. Hernández, C. Hernando, B. Jalžić, J. Král, K. Kunt, A. Kirin, M. Kuntner, A. López, H. Lopez, M. Lukić, N. Macías, J. Malumbres-Olarte, P. Marcia, Y. Marusik, M. Mejía, K. Miculinić, I. Napotnik, G. Nardi, P. Oromí, R. Ozimec, J. Pons, T. Rađa, P. Rade, N. Raguž, M. Rezač, C. Ribera, T. Rožman, T. Rubinić, A. Serra,

F. Stahlavsky, V. Sudar, S. Taiti, N. Txasko, C. J. Vink and M. Zapparoli. Special thanks are due to Raquel Alvarez, Alba Enguídanos, Mercè Loukota and Paola Mazzuca, who took part in the molecular work. Special thanks go to the organizations and individuals responsible for issuing the collecting and exporting permits for the specimens analysed. Ivan Magalhaes and anonymous reviewers deserve our gratitude for their insightful comments that significantly enhanced previous versions of the manuscript.

Conflict of interest

The authors declare no conflicts of interest.

References

Adrián-Serrano, S., Lozano-Fernandez, J., Pons, J., Rozas, J. and Arnedo, M.A., 2021. On the shoulder of giants: mitogenome recovery from non-targeted genome projects for phylogenetic inference and molecular evolution studies. J. Zool. Syst. Evol. Res. 59, 5–30.

Alicata, P., 1966. Le *Harpactea* della fauna italiana e considerazioni sulla loro origine. Atti dell' Accademia Gioenia di Scienze Naturali in Catania 18, 190–221.

Arnedo, M., Gasparo, F. and Opatova, V., 2009. Systematics and phylogeography of the *Dysdera erythrina* species complex (Araneae, Dysderidae) in Sardinia. ZooKeys 16, 319–345. https://doi.org/10.3897/zookeys.16.128

Arnedo, M.A., Oromí, P. and Ribera, C., 2001. Radiation of the spider genus *Dysdera* (Araneae, Dysderidae) in the Canary Islands: cladistic assessment based on multiple data sets. Cladistics 17, 313–353.

Arnedo, M.A., Oromí, P., Múrria, C., Macías-Hernández, N. and Ribera, C., 2007. The dark side of an island radiation: systematics and evolution of troglobitic spiders of the genus *Dysdera* Latreille (Araneae: Dysderidae) in the Canary Islands. Invertebr. Syst. 21, 623–660.

Austad, S.N., 1984. Evolution of sperm priority patterns in spiders. In: Smith, R.L. (Ed.), Sperm Competition and the Evolution of Mating Systems. Orlando, FL: Academic Press, pp. 223–249.

Baele, G., Li, W.L.S., Drummond, A.J., Suchard, M.A. and Lemey, P., 2013. Accurate model selection of relaxed molecular clocks in Bayesian phylogenetics. Mol. Biol. Evol. 30, 239–243.

Ballarin, F. and Li, S., 2018. Diversification in tropics and subtropics following the mid-Miocene climate change: a case study of the spider genus *Nesticella*. Glob. Chang. Biol. 24, e577–e591.

Barabás, G., Parent, C., Kraemer, A., Van de Perre, F. and De Laender, F., 2022. The evolution of trait variance creates a tension between species diversity and functional diversity. Nat. Commun. 13, 2521.

Bellvert, A., Adrián-Serrano, S., Macías-Hernández, N., Toft, S., Kaliontzopoulou, A. and Arnedo, M.A., 2023. The non-dereliction in evolution: trophic specialisation drives convergence in the radiation of red devil spiders (Araneae: Dysderidae) in the Canary Islands. Syst. Biol. 72, 998–1012.

Bergsten, J., 2005. A review of long-branch attraction. Cladistics 21, 163–193.

Bidegaray-Batista, L. and Arnedo, M.A., 2011. Gone with the plate: the opening of the Western Mediterranean Basin drove the diversification of ground-dweller spiders. BMC Evol. Biol. 11, 317.

Bidegaray-Batista, L., Ferrández, M.Á. and Arnedo, M.A., 2014. Winter is coming: Miocene and Quaternary climatic shifts shaped the diversification of Western-Mediterranean *Harpactocrates* (Araneae, Dysderidae) spiders. Cladistics 30, 428–446.

Borchsenius, F., 2009. FastGap 1.2.

Botsyun, S., Ehlers, T.A., Koptev, A., Böhme, M., Methner, K., Risi, C., Stepanek, C., Mutz, S.G., Werner, M., Boateng, D. and Mulch, A., 2022. Middle Miocene climate and stable oxygen isotopes in Europe based on numerical modeling. Paleoceanogr. Paleoclimatol. 37, 1–30. https://doi.org/10.1029/2022PA004442.

Bouckaert, R., Vaughan, T.G., Barido-Sottani, J., Duchêne, S., Fourment, M., Gavryushkina, A., Heled, J., Jones, G., Kühnert, D., De Maio, N., Matschiner, M., Mendes, F.K., Müller, N.F., Ogilvie, H.A., Du Plessis, L., Popinga, A., Rambaut, A., Rasmussen, D., Siveroni, I., Suchard, M.A., Wu, C.H., Xie, D., Zhang, C., Stadler, T. and Drummond, A.J., 2019. BEAST 2.5: an advanced software platform for Bayesian evolutionary analysis. PLoS Comput. Biol. 15, e1006650.

Brignoli, P.M., 1978. Ragni di Turchia V. Specie nuove o interessanti, cavernicole ed epigee, di varie famiglie (Araneae). Rev. Suisse Zool. 85, 461–541.

Britton, T., Anderson, C.L., Jacquet, D., Lundqvist, S. and Bremer, K., 2007. Estimating divergence times in large phylogenetic trees. Syst. Biol. 56, 741–752.

Burger, M. and Kropf, C., 2007. Genital morphology of the haplogyne spider *Harpactea lepida* (Arachnida, Araneae, Dysderidae). Zoomorphology 126, 45–52.

Capella-Gutiérrez, S., Silla-Martínez, J.M. and Gabaldón, T., 2009. trimAl: a tool for automated alignment trimming in large-scale phylogenetic analyses. Bioinformatics 25, 1972–1973.

Carracedo, J.C. and Day, S., 2002. Canary Islands. Terra Publishing, Harpenden, Hertfordshire, UK.

Ceccarelli, S.F., Koch, N.M., Soto, E.M., Barone, M.L., Arnedo, M.A. and Ramírez, M.J., 2019. The grass was greener: repeated evolution of specialized morphologies and habitat shifts in ghost spiders following grassland expansion in South America. Syst. Biol. 68, 63–77.

Chatzaki, M. and Arnedo, M.A., 2006. Taxonomic revision of the epigean representatives of the spider subfamily Harpacteinae (Araneae: Dysderidae) on the island of Crete. Zootaxa 1169, 1–32.

Chernomor, O., Von Haeseler, A. and Minh, B.Q., 2016. Terrace aware data structure for phylogenomic inference from supermatrices. Syst. Biol. 65, 997–1008.

Colgan, D.J., McLauchlan, A., Wilson, G.D.F., Livingston, S.P., Edgecombe, G.D., Macaranas, J., Cassis, G. and Gray, M.R., 1998. Histone H3 and U2 snRNA DNA sequences and arthropod molecular evolution. Aust. J. Zool. 46, 419–437.

Cooke, J.A.L., 1965. Spider genus *Dysdera* (Araneae, Dysderidae). Nature 205, 1027–1028.

Cooke, J.A.L., 1966. Synopsis of the structure and function of the genitalia in *Dysdera crocata*. Senckenberg. Biol. 47, 35–43.

Crespo, L.C., Silva, I., Enguídanos, A., Cardoso, P. and Arnedo, M.A., 2021a. Integrative taxonomic revision of the woodlouse-hunter spider genus *Dysdera* (Araneae: Dysderidae) in the Madeira archipelago with notes on its conservation status. Zool. J. Linnean Soc. 192, 356–415.

Crespo, L.C., Silva, I., Enguídanos, A., Cardoso, P. and Arnedo, M.A., 2021b. The Atlantic connection: coastal habitat favoured long distance dispersal and colonization of Azores and Madeira by *Dysdera* spiders (Araneae: Dysderidae). Syst. Biodivers. 19, 906–927.

Csiki-Sava, Z., Buffetaut, E., Ősi, A., Pereda-Suberbiola, X. and Brusatte, S.L., 2015. Island life in the Cretaceous—Faunal composition, biogeography, evolution, and extinction of landliving vertebrates on the Late Cretaceous European archipelago. ZooKeys 469, 1–161.

Culver, D.C. and Sket, B., 2000. Hotspots of subterranean biodiversity in caves and wells. J. Cave Karst Stud. 62, 11–17.

Deeleman-Reinhold, C.L., 1993. The genus Rhode and the Harpacteine genera *Stalagtia*, *Folkia*, *Minotauria*, and *Kaemis*

(Araneae, Dysderidae) of Yugoslavia and Crete, with remarks on the genus *Harpactea*. Revue Arachnol. 10, 105–135.
Deeleman-Reinhold, C.L. and Deeleman, P.R., 1988. Revision des Dysderinae les especes mediterraneennes occidentales exceptees. Tijdschrift voor Entomol. 131, 141–269.
Deltshev, C., 1999. A faunistic and zoogeographical review of the spiders (Araneae) of the Balkan Peninsula. J. Arachnol. 27, 255–261.
Deltshev, C., 2011. *Harpactea lazarovi* sp. n. and *H. tenuiemboli* sp. n., two new spider species from Balkan Peninsula (Araneae, Dysderidae). Zoosyst. Evol. 87, 221–226.
Felsenstein, J., 2004. Inferring Phylogenies. Sinauer Associates, Sunderland, Massachusetts.
Fernández, R., Kallal, R.J., Dimitrov, D., Ballesteros, J.A., Arnedo, M.A., Giribet, G. and Hormiga, G., 2018. Phylogenomics, diversification dynamics, and comparative transcriptomics across the spider tree of life. Curr. Biol. 28, 1489–1497.e5.
Fleischer, R.C., McIntosh, C.E. and Tarr, C.L., 1998. Evolution on a volcanic conveyor belt: using phylogeographic reconstructions and K-Ar-based ages of the Hawaiian Islands to estimate molecular evolutionary rates. Mol. Ecol. 7, 533–545.
Folmer, O., Black, M., Hoeh, W., Lutz, R. and Vrijenhoek, R., 1994. DNA primers for amplification of mitochondrial cytochrome c oxidase subunit I from diverse metazoan invertebrates. Mol. Mar. Biol. Biotechnol. 3, 294–299.
Forster, R.R. and Platnick, N.I., 1985. A review of the austral spider family Orsolobidae (Arachnida, Araneae), with notes on the superfamily Dysderoidea. Bull. Am. Mus. Nat. Hist. 181, 1–230.
Garrison, N.L., Rodriguez, J., Agnarsson, I., Coddington, J.A., Griswold, C.E., Hamilton, C.A., Hedin, M., Kocot, K.M., Ledford, J.M. and Bond, J.E., 2016. Spider phylogenomics: untangling the spider tree of life. PeerJ 4, e1719.
Geer, L.Y., Marchler-Bauer, A., Geer, R.C., Han, L., He, J., He, S., Liu, C., Shi, W. and Bryant, S.H., 2010. The NCBI BioSystems database. Nucleic Acids Res. 38, 492–496.
Geller, J., Meyer, C., Parker, M. and Hawk, H., 2013. Redesign of PCR primers for mitochondrial cytochrome c oxidase subunit I for marine invertebrates and application in all-taxa biotic surveys. Mol. Ecol. Resour. 13, 851–861.
Giribet, G., Carranza, S., Baguñà, J., Riutort, M. and Ribera, C., 1996. First molecular evidence for the existence of a Tardigrada + Arthropoda clade. Mol. Biol. Evol. 13, 76–84.
Giribet, G., Edgecombe, G.D. and Wheeler, W.C., 1999. Sistemática y filogenia de artrópodos: estado de la cuestión con énfasis en el análisis de datos moleculares. Boletín de la Sociedad Entomológica Aragonesa 26, 197–212.
Goloboff, P.A. and Catalano, S.A., 2016. TNT version 1.5, including a full implementation of phylogenetic morphometrics. Cladistics 32, 221–238.
Guindon, S., Dufayard, J.F., Lefort, V., Anisimova, M., Hordijk, W. and Gascuel, O., 2010. New algorithms and methods to estimate maximum-likelihood phylogenies: assessing the performance of PhyML 3.0. Syst. Biol. 59, 307–321.
Heads, M., 2011. Old taxa on young Islands: a critique of the use of island age to date island-endemic clades and calibrate phylogenies. Syst. Biol. 60, 204–218.
Hedin, M.C. and Maddison, W.P., 2001. A combined molecular approach to phylogeny of the jumping spider subfamily Dendryphantinae (Araneae: Salticidae). Mol. Phylogenet. Evol. 18, 386–403.
Hendy, M.D., 1989. The relationship between simple evolutionary tree models and observable sequence data. Syst. Zool. 38, 310–321.
Hipsley, C.A. and Müller, J., 2014. Beyond fossil calibrations: realities of molecular clock practices in evolutionary biology. Front. Genet. 5, 1–11. https://doi.org/10.3389/fgene.2014.00138.
Ho, S.Y.W. and Phillips, M.J., 2009. Accounting for calibration uncertainty in phylogenetic estimation of evolutionary divergence times. Syst. Biol. 58, 367–380.
Hopkin, S.P. and Martin, M.H., 1985. Assimilation of zinc, cadmium, lead, copper, and iron by the spider *Dysdera crocata*, a predator of woodlice. Bull. Environ. Contam. Toxicol. 34, 183–187.
Huelsenbeck, J.P., 1998. Systematic bias in phylogenetic analysis: is the Strepsiptera problem solved? Syst. Biol. 47, 519–537.
Kallal, R.J., Kulkarni, S.S., Dimitrov, D., Benavides, L.R., Arnedo, M.A., Giribet, G. and Hormiga, G., 2021. Converging on the orb: denser taxon sampling elucidates spider phylogeny and new analytical methods support repeated evolution of the orb web. Cladistics 37, 298–316.
Kass, R.E. and Raftery, A.E., 1995. Bayes factors. J. Am. Stat. Assoc. 90, 773–795.
Katoh, K., Rozewicki, J. and Yamada, K.D., 2019. MAFFT online service: Multiple sequence alignment, interactive sequence choice and visualization. Brief. Bioinform. 20, 1160–1166.
Kearse, M., Moir, R., Wilson, A., Stones-Havas, S., Cheung, M., Sturrock, S., Buxton, S., Cooper, A., Markowitz, S., Duran, C., Thierer, T., Ashton, B., Meintjes, P. and Drummond, A., 2012. Geneious Basic: an integrated and extendable desktop software platform for the organization and analysis of sequence data. Bioinformatics 28, 1647–1649.
Kolaczkowski, B. and Thornton, J.W., 2004. Performance of maximum parsimony and likelihood phylogenetics when evolution is heterogeneous. Nature 431, 980–984.
Král, J., Musilová, J., Šťáhlavský, F., Řezáč, M., Akan, Z., Edwards, R.L., Coyle, F.A. and Almerje, C.R., 2006. Evolution of the karyotype and sex chromosome systems in basal clades of araneomorph spiders (Araneae: Araneomorphae). Chromosom. Res. 14, 859–880.
Kulkarni, S., Kallal, R.J., Wood, H., Dimitrov, D., Giribet, G. and Hormiga, G., 2021. Interrogating genomic-scale data to resolve recalcitrant nodes in the spider tree of life. Mol. Biol. Evol. 38, 891–903.
Kulkarni, S., Wood, H.M. and Hormiga, G., 2023. Advances in the reconstruction of the spider tree of life: a roadmap for spider systematics and comparative studies. Cladistics 39, 479–532.
Labarque, F.M., Pérez-González, A. and Griswold, C.E., 2018. Molecular phylogeny and revision of the false violin spiders (Araneae: Drymusidae) of Africa. Zool. J. Linnean Soc. 183, 390–430.
Lanfear, R., Frandsen, P.B., Wright, A.M., Senfeld, T. and Calcott, B., 2017. Partitionfinder 2: new methods for selecting partitioned models of evolution for molecular and morphological phylogenetic analyses. Mol. Biol. Evol. 34, 772–773.
Leray, M., Yang, J.Y., Meyer, C.P., Mills, S.C., Agudelo, N., Ranwez, V., Boehm, J.T. and Machida, R.J., 2013. A new versatile primer set targeting a short fragment of the mitochondrial COI region for metabarcoding metazoan diversity: application for characterizing coral reef fish gut contents. Front. Zool. 10, 34.
Lockhart, P. and Steel, M., 2005. A tale of two processes. Syst. Biol. 54, 948–951.
Lockhart, P., Novis, P., Milligan, B.G., Riden, J., Rambaut, A. and Larkum, T., 2006. Heterotachy and tree building: a case study with plastids and eubacteria. Mol. Biol. Evol. 23, 40–45.
Lopez, P., Casane, D. and Philippe, H., 2002. Heterotachy, an important process of protein evolution. Mol. Biol. Evol. 19, 1–7.
Macías-Hernández, N., Oromí, P. and Arnedo, M.A., 2008. Patterns of diversification on old volcanic islands as revealed by the woodlouse-hunter spider genus *Dysdera* (Araneae, Dysderidae) in the eastern Canary Islands. Biol. J. Linn. Soc. 94, 589–615.
Macías-Hernández, N., Oromí, P. and Arnedo, M.A., 2010. Integrative taxonomy uncovers hidden species diversity in woodlouse hunter spiders (Araneae, Dysderidae) endemic to the Macaronesian archipelagos. Syst. Biodivers. 8, 531–553.
Macías-Hernández, N., López, S.C., Roca-Cusachs, M., Oromí, P. and Arnedo, M.A., 2016. A geographical distribution database of the genus *Dysdera* in the Canary Islands (Araneae, Dysderidae). ZooKeys 2016, 11–23.
Magalhaes, I.L.F., Azevedo, G.H.F., Michalik, P. and Ramírez, M.J., 2020. The fossil record of spiders revisited: implications for

calibrating trees and evidence for a major faunal turnover since the Mesozoic. Biol. Rev. 95, 184–217.
Magalhaes, I.L.F., Pérez-González, A., Labarque, F.M., Carboni, M., Hammel, J.U., Kunz, R., Ramírez, M.J. and Solórzano-Kraemer, M.M., 2022. Revision of recluse spiders (Araneae: Sicariidae: *Loxosceles*) preserved in Dominican amber and a totalevidence phylogeny of Scytodoidea reveal the first fossil Drymusidae. Arthropod Syst. Phylogeny 80, 541–559.
Mammola, S., Isaia, M. and Arnedo, M.A., 2015. Alpine endemic spiders shed light on the origin and evolution of subterranean species. PeerJ 2015, e1384.
Mammola, S., Cardoso, P., Ribera, C., Pavlek, M. and Isaia, M., 2018. A synthesis on cave-dwelling spiders in Europe. J. Zool. Syst. Evol. Res. 56, 301–316.
McIntyre, S.R.N., Lineweaver, C.H., Groves, C.P. and Chopra, A., 2017. Global biogeography since Pangaea. Proc. R. Soc. B Biol. Sci. 284, 20170716.
Meyer, A.L.S., Román-Palacios, C. and Wiens, J.J., 2018. BAMM gives misleading rate estimates in simulated and empirical datasets. Evolution 72, 2257–2266.
Michalik, P. and Ramírez, M.J., 2014. Evolutionary morphology of the male reproductive system, spermatozoa and seminal fluid of spiders (Araneae, Arachnida)—current knowledge and future directions. Arthropod Struct. Dev. 43, 291–322.
Michalik, P., Dallai, R., Giusti, F. and Alberti, G., 2004. The ultrastructure of the peculiar synspermia of some Dysderidae (Araneae, Arachnida). Tissue Cell 36, 447–460.
Michalik, P., Kallal, R., Dederichs, T.M., Labarque, F.M., Hormiga, G., Giribet, G. and Ramírez, M.J., 2019. Phylogenomics and genital morphology of cave raptor spiders (Araneae, Trogloraptoridae) reveal an independent origin of a flow-through female genital system. J. Zool. Syst. Evol. Res. 57, 737–747.
Miller, M.A., Pfeiffer, W. and Schwartz, T., 2010. Creating the CIPRES Science Gateway for inference of large phylogenetic trees. 2010 Gateway Computing Environments Workshop (GCE), 1–8.
Moore, B.R., Höhna, S., May, M.R., Rannala, B. and Huelsenbeck, J.P., 2016. Critically evaluating the theory and performance of Bayesian analysis of macroevolutionary mixtures. PNAS 113, 9569–9574.
Nguyen, L.T., Schmidt, H.A., Von Haeseler, A. and Minh, B.Q., 2015. IQ-TREE: a fast and effective stochastic algorithm for estimating maximum-likelihood phylogenies. Mol. Biol. Evol. 32, 268–274.
Pekár, S., Líznarová, E. and Řezáč, M., 2016. Suitability of woodlice prey for generalist and specialist spider predators: a comparative study. Ecol. Entomol. 41, 123–130.
Philippe, H., Delsuc, F., Brinkmann, H. and Lartillot, N., 2005. Phylogenomics. Annu. Rev. Ecol. Evol. Syst. 36, 541–562.
Platania, L., Pavlek, M. and Arnedo, M., 2020. Testing the monophyly of the ground-dweller spider genus *Harpactea* Bristowe, 1939 (Araneae, Dysderidae) with the description of three new species. Syst. Biodivers. 18, 688–707.
Platnick, N.I., Coddington, J.A., Forster, R.R. and Griswold, C.E., 1991. Spinneret morphology and the phylogeny of haplogyne spiders (Araneae, Araneomorphae). Am. Mus. Novit. 3016, 1–73.
Pol, D. and Siddall, M.E., 2001. Biases in maximum likelihood and parsimony: a simulation approach to a 10-taxon case. Cladistics 17, 266–281.
Pons, J. and Vogler, A.P., 2006. Size, frequency, and phylogenetic signal of multiple-residue indels in sequence alignment of introns. Cladistics 22, 144–156.
Prothero, D.R. and Berggren, W.A., 1992. Eocene-Oligocene Climatic and Biotic Evolution. Princeton, NJ: Princeton University Press.
Rabosky, D.L., 2014. Automatic detection of key innovations, rate shifts, and diversity-dependence on phylogenetic trees. PLoS One 9, e89543.
Rabosky, D.L., Grundler, M., Anderson, C., Title, P., Shi, J.J., Brown, J.W., Huang, H. and Larson, J.G., 2014. BAMMtools: an R package for the analysis of evolutionary dynamics on phylogenetic trees. Methods Ecol. Evol. 5, 701–707.
Rabosky, D.L., Mitchell, J.S. and Chang, J., 2017. Is BAMM flawed? Theoretical and practical concerns in the analysis of multi-rate diversification models. Syst. Biol. 66, 477–498. https://doi.org/10.1093/sysbio/syx037.
Rambaut, A., 2009. FigTree, version 1.4.3. Computer program distributed by the author. http://tree.bio.ed.ac.uk/software/figtree/ [accessed November 16, 2023].
Rambaut, A., Drummond, A.J., Xie, D., Baele, G. and Suchard, M.A., 2018. Posterior summarization in Bayesian phylogenetics using Tracer 1.7. Syst. Biol. 67, 901–904.
Ramírez, M.J., 2000. Respiratory system morphology and the phylogeny of haplogyne spiders (Araneae, Araneomorphae). J. Arachnol. 28, 149–157.
Ramírez, M.J., Magalhaes, I.L.F., Derkarabetian, S., Ledford, J., Griswold, C.E., Wood, H.M. and Hedin, M., 2021. Sequence capture phylogenomics of true spiders reveals convergent evolution of respiratory systems. Syst. Biol. 70, 14–20.
Řezáč, M. and Pekár, S., 2007. Evidence for woodlice-specialization in *Dysdera* spiders: behavioural versus developmental approaches. Physiol. Entomol. 32, 367–371.
Řezáč, M., Král, J. and Pekár, S., 2007. The spider genus *Dysdera* (Araneae, Dysderidae) in central Europe: revision and natural history. J. Arachnol. 35, 432–462.
Řezáč, M., Pekár, S. and Lubin, Y., 2008. How oniscophagous spiders overcome woodlouse armour. J. Zool. 275, 64–71.
Řezáč, M., Arnedo, M.A., Opatova, V., Musilová, J., Řezáčová, V. and Král, J., 2018. Taxonomic revision and insights into the speciation mode of the spider *Dysdera erythrina* species-complex (Araneae : Dysderidae): Sibling species with sympatric distributions. Invertebr. Syst. 32, 10–54.
Řezáč, M., Pekár, S., Arnedo, M., Macías-Hernández, N. and Řezáčová, V., 2021. Evolutionary insights into the eco-phenotypic diversification of *Dysdera* spiders in the Canary Islands. Org. Divers. Evol. 21, 79–92.
Ribeiro, P.L., Rapini, A., Silva, U.C.S. and Berg, C., 2012. Using multiple analytical methods to improve phylogenetic hypotheses in *Minaria* (Apocynaceae). Mol. Phylogenet. Evol. 65, 915–925.
Ribera, C., 2004. *Dysdera valentina* (Araneae, Dysderidae), una nueva especie de la provincia de Valencia, con algunas adiciones a la fauna cavernícola ibérica. Revista Ibérica de Aracnología 9, 211–215.
Ribera, C. and Arnedo, M.A., 1994. Description of *Dysdera gollumi* (Araneae, Haplogynae), a new troglobitic species from Tenerife, Canary Islands, with some comments on Canarian *Dysdera*. Mémories de Biospéologie 21, 115–119.
Ronquist, F. and Huelsenbeck, J.P., 2003. MrBayes 3: Bayesian phylogenetic inference under mixed models. Bioinformatics 19, 1572–1574.
Rosenbaum, G., Lister, G.S. and Duboz, C., 2002. Reconstruction of the tectonic evolution of the western Mediterranean since the Oligocene. J. Virtual Explor. 8, 107–126.
Schettino, A. and Turco, E., 2006. Plate kinematics of the Western Mediterranean region during the Oligocene and Early Miocene. Geophys. J. Int. 166, 1398–1423.
Selden, P.A., Shear, W.A. and Sutton, M.D., 2008. Fossil evidence for the origin of spider spinnerets, and a proposed arachnid order. Proc. Natl. Acad. Sci. 105, 20781–20785.
Seton, M., Gaina, C., Müller, R.D. and Heine, C., 2009. Mid-Cretaceous seafloor spreading pulse: fact or fiction? Geology 37, 687–690.
Shao, L. and Li, S., 2018. Early Cretaceous greenhouse pumped higher taxa diversification in spiders. Mol. Phylogenet. Evol. 127, 146–155.
Siddall, M.E. and Whiting, M.F., 1999. Long-branch abstractions. Cladistics 15, 9–24.
Simmons, M.P. and Ochoterena, H., 2000. Gaps as characters in sequence-based phylogenetic analyses. Syst. Biol. 49, 369–381.
Simmons, M.P., Zhang, L.B., Webb, C.T., Reeves, A. and Miller, J.A., 2006. The relative performance of Bayesian and parsimony approaches when sampling characters evolving under homogeneous and heterogeneous sets of parameters. Cladistics 22, 171–185.

Simon, C., Frati, F., Beckenbach, A., Crespi, B., Hong, L. and Paul, F., 1994. Evolution weighting and phylogenetic utility of mitochondrial gene sequences and a compilation of conserved polymerase chain reaction primers. Ann. Entomol. Soc. Am. 87, 651–701.
Siravo, G., Speranza, F. and Mattei, M., 2023. Paleomagnetic evidence for Pre-21 Ma independent drift of South Sardinia from North Sardinia-Corsica: "Greater Iberia" versus Europe. Tectonics 42, 1–15. https://doi.org/10.1029/2022TC007705.
Spencer, M., Susko, E. and Roger, A.J., 2005. Likelihood, parsimony, and heterogeneous evolution. Mol. Biol. Evol. 22, 1161–1164.
Stamatakis, A., 2006. Phylogenetic models of rate heterogeneity: a high performance computing perspective. In: Proceedings 20th IEEE International Parallel & Distributed Processing Symposium, Rhodes, Greece, p. 8. https://doi.org/10.1109/IPDPS.2006.1639535.
Stamatakis, A., 2014. RAxML version 8: a tool for phylogenetic analysis and post-analysis of large phylogenies. Bioinformatics 30, 1312–1313.
Talavera, G., Lukhtanov, V.A., Pierce, N.E. and Vila, R., 2013. Establishing criteria for higher-level classification using molecular data: the systematics of *Polyommatus* blue butterflies (Lepidoptera, Lycaenidae). Cladistics 29, 166–192.
Thi Hoang, D., Chernomor, O., von Haeseler, A., Quang Minh, B., Sy Vinh, L. and Rosenberg, M.S., 2018. UFBoot2: improving the ultrafast bootstrap approximation. Mol. Biol. Evol. 35, 518–522.
Thornton, J.W. and Kolaczkowski, B., 2005. No magic pill for phylogenetic error. Trends Genet. 21, 310–311.
Toft, S. and Macías-Hernández, N., 2017. Metabolic adaptations for isopod specialization in three species of *Dysdera* spiders from the Canary Islands. Physiol. Entomol. 42, 191–198.
Tuf, I.H. and Ďurajková, B., 2022. Antipredatory strategies of terrestrial isopods. ZooKeys 1101, 109–129.
Uhl, G., 2000a. Two distinctly different sperm storage organs in female *Dysdera erythrina* (Araneae: Dysderidae). Arthropod Struct. Dev. 29, 163–169.
Uhl, G., 2000b. Female genital morphology and sperm priority patterns in spiders (Araneae). In: Proceedings of the 19th European Colloquium of Arachnology. Aarhus: Aarhus University Press, pp. 145–156.
Vizueta, J., Macías-Hernández, N., Arnedo, M.A., Rozas, J. and Sánchez-Gracia, A., 2019. Chance and predictability in evolution: the genomic basis of convergent dietary specializations in an adaptive radiation. Mol. Ecol. 28, 4028–4045.
Wheeler, W.C., 1995. Sequence alignment, parameter sensitivity, and the phylogenetic analysis of molecular data. Syst. Biol. 44, 321–331.
Wheeler, W.C., Coddington, J.A., Crowley, L.M., Dimitrov, D., Goloboff, P.A., Griswold, C.E., Hormiga, G., Prendini, L., Ramírez, M.J., Sierwald, P., Almeida-Silva, L., Alvarez-Padilla, F., Arnedo, M.A., Benavides Silva, L.R., Benjamin, S.P., Bond, J.E., Grismado, C.J., Hasan, E., Hedin, M., Izquierdo, M.A., Labarque, F.M., Ledford, J., Lopardo, L., Maddison, W.P., Miller, J.A., Piacentini, L.N., Platnick, N.I., Polotow, D., Silva-Dávila, D., Scharff, N., Szűts, T., Ubick, D., Vink, C.J., Wood, H.M. and Zhang, J., 2017. The spider tree of life: phylogeny of Araneae based on target-gene analyses from an extensive taxon sampling. Cladistics 33, 574–616.
White, W.B. and Culver, D.C., 2007. Encyclopedia of Caves, 1st edition, Waltham, MA: Academic Press.
World Spider Catalog, 2023. World Spider Catalog. Version 24.5. [WWW Document]. Natural History Museum Bern. http://wsc.nmbe.ch, accessed on (accessed 10.6.23).

Supporting Information

Additional supporting information may be found online in the Supporting Information section at the end of the article.

Fig. S1 The 12s maximum likelihood tree obtained with IQtree.

Fig. S2 The 16s maximum likelihood tree obtained with IQtree.

Fig. S3 The 18s maximum likelihood tree obtained with IQtree.

Fig. S4 The 28s maximum likelihood tree obtained with IQtree.

Fig. S5 The cox1 maximum likelihood tree obtained with IQtree.

Fig. S6 The h3 maximum likelihood tree obtained with IQtree.

Fig. S7 The concatenated maximum likelihood tree obtained with IQtree without removing missing data.

Fig. S8 The concatenated maximum likelihood tree obtained with IQtree after removing columns with more than 75% gaps in the alignment.

Fig. S9 The concatenated maximum likelihood tree obtained with IQtree after removing columns with more than 50% gaps in the alignment.

Fig. S10 The concatenated maximum likelihood tree obtained with IQtree after removing columns with more than 25% gaps in the alignment.

Fig. S11 The concatenated parsimony tree with gaps coded as missing data.

Fig. S12 The concatenated parsimony tree with gaps coded as absence/presence.

Fig. S13 The concatenated maximum likelihood tree obtained with IQtree.

Fig. S14 The concatenated maximum likelihood tree obtained with RAxML.

Fig. S15 The concatenated Bayesian inference tree on six partitions scheme.

Fig. S16 The concatenated Bayesian inference tree on 10 partitions scheme.

Fig. S17 The chronogram inferred with BEAST using both fossil and biogeographic calibration points.

Fig. S18 The chronogram inferred with BEAST using only fossil calibration points.

Fig. S19 Comparison of dates inferred for the main clades using both fossil and biogeographic calibration points (black) or only fossil calibration points (grey).

Table S1 Specimens included in the study.

Table S2 Primer sequences used for amplification and sequencing.

Table S3 PCR profiles for amplification.

Table S4 Sequencing information and alignment composition.

Table S5 Partition schemes and scores for the tree inference.

Table S6 Best nucleotide evolution model for each partition and scheme for the tree inference.

Table S7 Information on calibration points used for node-dating.

Table S8 Partition schemes and scores for the timetree estimation.

Table S9 Best nucleotide evolution models for each partition and scheme for the timetree estimation.

Table S10 Prior model comparison for the dating analysis based on Bayes factor.

Table S11 Dysderidae species estimate for BAMM diversification analyses.

Table S12 BAMM model probabilities.

Table S13 BAMM model comparison based on Bayes factors.

Table S14 Estimated speciation and extinction rates in BAMM.